AD-A174 679 PH-SENSITIVE NI(OH)2-BASED MICROELECTROCHEMICAL TRANSISTORS(U) MASSACHUSETTS INST OF TECH CAMBRIDGE DEPT OF CHEMISTRY M J NATAN ET AL 24 NOV 86 1/1

UNCLASSIFIED N00014-84-K-0553 F/G 9/1 NL

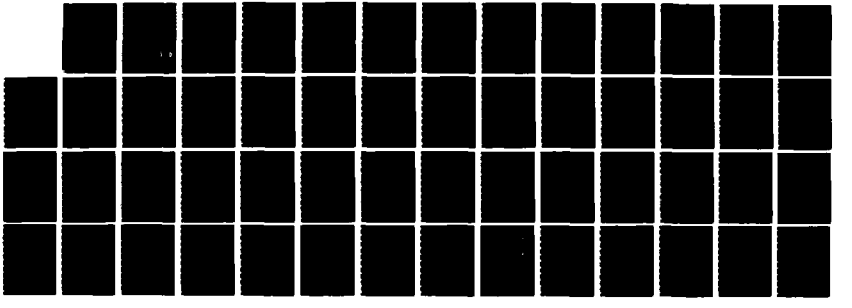

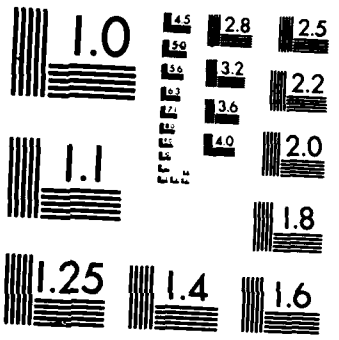

SECURITY CLASSIFICATION OF THIS PAGE

REPOR

1a. REPORT SECURITY CLASSIFICATION: unclassified

AD-A174 679

e

2a. SECURITY CLASSIFICATION AUTHORITY

REPORT

2b. DECLASSIFICATION / DOWNGRADING SCHEDULE: unlimited

4. PERFORMING ORGANIZATION REPORT NUMBER(S)

5. MONITORING ORGANIZATION REPORT NUMBER(S): N00014-84-K-0553 and N00014-84-K-0291

6a. NAME OF PERFORMING ORGANIZATION: M.I.T.

6b. OFFICE SYMBOL (*If applicable*)

7a. NAME OF MONITORING ORGANIZATION: Office of Naval Research

6c. ADDRESS (*City, State, and ZIP Code*): Department of Chemistry, Massachusetts Institute of Technology, Cambridge, MA 02139

7b. ADDRESS (*City, State, and ZIP Code*)

8a. NAME OF FUNDING / SPONSORING ORGANIZATION: Office of Naval Research

8b. OFFICE SYMBOL (*If applicable*)

9. PROCUREMENT INSTRUMENT IDENTIFICATION NUMBER

8c. ADDRESS (*City, State, and ZIP Code*): Department of the Navy, Arlington, VA 22217

10. SOURCE OF FUNDING NUMBERS

PROGRAM ELEMENT NO.	PROJECT NO.	TASK NO.	WORK UNIT ACCESSION NO.
		051-579	202-261

11. TITLE (*Include Security Classification*): pH-Sensitive $Ni(OH)_2$-Based Microelectrochemical Transistors

12. PERSONAL AUTHOR(S): Michael J. Natan, D. Belanger, M.K. Carpenter and Mark S. Wrighton

13a. TYPE OF REPORT	13b. TIME COVERED FROM ____ TO ____	14. DATE OF REPORT (*Year, Month, Day*)	15. PAGE COUNT
interim		November 24, 1986	47

16. SUPPLEMENTARY NOTATION: Prepared for publication in the Journal of Physical Chemistry

17. COSATI CODES		
FIELD	GROUP	SUB-GROUP

18. SUBJECT TERMS (*Continue on reverse if necessary and identify by block number*): Molecular electronics, microelectrochemistry, pH-sensors, Chemical sensors, electroactive oxides

19. ABSTRACT (*Continue on reverse if necessary and identify by block number*)

See attached

20. DISTRIBUTION / AVAILABILITY OF ABSTRACT
☐ UNCLASSIFIED/UNLIMITED ☐ SAME AS RPT. ☐ DTIC USERS

21. ABSTRACT SECURITY CLASSIFICATION

22a. NAME OF RESPONSIBLE INDIVIDUAL: Mark S. Wrighton

22b. TELEPHONE (*Include Area Code*): 617-253-1597

22c. OFFICE SYMBOL

DD FORM 1473, 84 MAR

83 APR edition may be used until exhausted.
All other editions are obsolete.

SECURITY CLASSIFICATION OF THIS PAGE

Abstract

Properties of arrays of closely spaced (1.2 μm) Au or Pt microelectrodes (~2 μm wide x 50 μm long x 0.1 μm high) coated with cathodically grown films of $Ni(OH)_2$ are reported. Electrical connection of microelectrodes by $Ni(OH)_2$ was verified by cyclic voltammetry. The ratio of anodic charge to cathodic charge in cyclic voltammograms for the $Ni(OH)_2 \rightleftharpoons NiO(OH)$ interconversion exceeds one. However, it is shown that excess charge in the anodic cyclic voltammetric wave for oxidation of $Ni(OH)_2$ does not affect the conductivity of $Ni(OH)_2$ films. The steady state resistance of $Ni(OH)_2$ connecting two microelectrodes has been measured as a function of potential from 0 V to 0.7 V vs. SCE, and was typically found to vary from ~10^7 to ~10^4 ohms. The measured resistance corresponds to a resistivity of approximately 30 ohm-cm in the oxidized state. The decrease in resistance is caused by electrochemical oxidation of insulating $Ni(OH)_2$ to "conducting" NiO(OH). At fixed drain voltage, V_D, the gate current, I_G, and the drain current, I_D, can be measured simultaneously as the gate voltage, V_G, is varied at a given frequency. The frequency response is limited by the slow electrochemistry of $Ni(OH)_2$ films. At a frequency of 3.8×10^{-2} Hz, $Ni(OH)_2$-based microelectrochemical transistors can amplify electrical power by a factor of 20. The temperature dependence of I_D indicates an activation energy for conductivity in NiO(OH) of 23 ± 2 kJ/mol at V_G = 0.45 V vs. SCE. A pair of microelectrodes connected by $Ni(OH)_2$ functions as a pH-sensitive microelectrochemical transistor, because there is a pH dependence in the potential associated with the oxidation of $Ni(OH)_2$. The pH dependence of the transistor behavior is

illustrated under dynamic and steady state conditions; as the pH of a basic solution is increased, V_G for device turn on moves negative, in accord with the known pH dependence of the redox chemistry of $Ni(OH)_2$. Detection of a change in pH from 12 to 13 in a flowing stream was demonstrated using $Ni(OH)_2$-based microelectrochemical transistors.

Accesion For	
NTIS CRA&I	☑
DTIC TAB	☐
Unannounced	☐
Justification	
By	
Distribution /	
Availability Codes	
Dist	Avail and / or Special
A-1	

OFFICE OF NAVAL RESEARCH

Contract N00014-84-K-0553
Task No. NR 051-579

and

Contract N00014-84-K-0291
Work Unit 202-261

pH-Sensitive $Ni(OH)_2$-Based Microelectrochemical Transistors

by

Michael J. Natan, Daniel Belanger, Michael K. Carpenter

and Mark S. Wrighton

Prepared for Publication

in the

Journal of Physical Chemistry

Massachusetts Institute of Technology
Department of Chemistry
Cambridge, Massachusetts

November 24, 1986

[Prepared for publication in the Journal of Physical Chemistry]
Revised form: November 10, 1986

pH-Sensitive $Ni(OH)_2$-Based Microelectrochemical Transistors

Michael J. Natan,[a] Daniel Bélanger,[a] Michael K. Carpenter,*[b] and Mark S. Wrighton*[a]

[a] Department of Chemistry
Massachusetts Institute of Technology
Cambridge, Massachusetts 02139

[b] Electrochemistry Department
General Motors Research Laboratories
Warren, Michigan 48090

*Address correspondence to these authors.

Abstract

Properties of arrays of closely spaced (1.2 μm) Au or Pt microelectrodes (~2 μm wide x 50 μm long x 0.1 μm high) coated with cathodically grown films of $Ni(OH)_2$ are reported. Electrical connection of microelectrodes by $Ni(OH)_2$ was verified by cyclic voltammetry. The ratio of anodic charge to cathodic charge in cyclic voltammograms for the $Ni(OH)_2 \rightleftharpoons NiO(OH)$ interconversion exceeds one. However, it is shown that excess charge in the anodic cyclic voltammetric wave for oxidation of $Ni(OH)_2$ does not affect the conductivity of $Ni(OH)_2$ films. The steady state resistance of $Ni(OH)_2$ connecting two microelectrodes has been measured as a function of potential from 0 V to 0.7 V vs. SCE, and was typically found to vary from $\sim 10^7$ to $\sim 10^4$ ohms. The measured resistance corresponds to a resistivity of approximately 30 ohm-cm in the oxidized state. The decrease in resistance is caused by electrochemical oxidation of insulating $Ni(OH)_2$ to "conducting" NiO(OH). At fixed drain voltage, V_D, the gate current, I_G, and the drain current, I_D, can be measured simultaneously as the gate voltage, V_G, is varied at a given frequency. The frequency response is limited by the slow electrochemistry of $Ni(OH)_2$ films. At a frequency of 3.8×10^{-2} Hz, $Ni(OH)_2$-based microelectrochemical transistors can amplify electrical power by a factor of 20. The temperature dependence of I_D indicates an activation energy for conductivity in NiO(OH) of 23 ± 2 kJ/mol at V_G = 0.45 V vs. SCE. A pair of microelectrodes connected by $Ni(OH)_2$ functions as a pH-sensitive microelectrochemical transistor, because there is a pH dependence in the potential associated with the oxidation of $Ni(OH)_2$. The pH dependence of the transistor behavior is

illustrated under dynamic and steady state conditions; as the pH of a basic solution is increased, V_G for device turn on moves negative, in accord with the known pH dependence of the redox chemistry of $Ni(OH)_2$. Detection of a change in pH from 12 to 13 in a flowing stream was demonstrated using $Ni(OH)_2$-based microelectrochemical transistors.

In this article we report the properties of pH-sensitive $Ni(OH)_2$-based microelectrochemical transistors, prepared by cathodic electrochemical deposition of $Ni(OH)_2$ onto Au or Pt microelectrode arrays. The oxidation of $Ni(OH)_2$, usually written as in equation (1),

$$Ni(OH)_2 \rightleftharpoons NiO(OH) + H^+ + e^- \qquad (1)$$

has been of great interest to electrochemists since the turn of the century, when Edison patented the use of $Ni(OH)_2$ as the anode in alkaline electrochemical storage cells. Since then, a tremendous amount of research has been devoted to understanding this complex reaction.[1,2] There are several methods of preparation of electroactive $Ni(OH)_2$ films, including direct growth from Ni metal electrodes[3] and electrodeposition onto conducting substrates by a variety of cathodic[4] or anodic[5] techniques. In addition to being an important battery electrode, $Ni(OH)_2$ is an electrochromic material, becoming colored upon electrochemical oxidation.[6] Like other electrochromic transition metal oxides,[7] coloration of $Ni(OH)_2$ is accompanied by a significant increase in conductivity. This change in conductivity, coupled with the pH dependence of the electrochemical potential where oxidation to the conducting state occurs, and the ability to derivatize $Ni(OH)_2$ on closely spaced (1.2 μm) microelectrodes, together provide the basis for a pH-dependent microelectrochemical transistor. In principle, any of the proton-dependent electrochromic transition metal oxides, such as WO_3,[7,8] Nb_2O_5,[7,9] IrO_2,[7,10] MoO_3,[7,11] or RhO_2,[7,12] that can be derivatized onto closely spaced microelectrodes should exhibit pH-dependent

transistor-like behavior. A study of pH-sensitive WO_3-based microelectrochemical transistors, prepared by rf plasma deposition of polycrystalline WO_3 onto microelectrode arrays, has been completed.[13]

Closely spaced (1.2 μm) Pt or Au microelectrodes (~2 μm wide x ~50 μm long x ~0.1 μm high) are useful to the study of the conductivity of transition metal oxides like $Ni(OH)_2$ and WO_3,[13] whose conductivities are low compared to metals. They have also been useful in the study of conducting, electroactive organic polymers that can be derivatized onto Pt or Au. Polypyrrole,[14] polyaniline,[15] and poly(3-methylthiophene)[16] all undergo conductivity changes accompanying electrochemical redox reactions of the polymers. Thus, microelectrochemical transistors based on conducting organic polymer-connected microelectrodes have already been demonstrated.[14-16] Derivatized microelectrode arrays have been also been useful in the demonstration of molecule-based diodes.[17,18]

Scheme I illustrates the operation of a microelectrochemical transistor based on conductivity modulation of $Ni(OH)_2$. The extent of oxidation (and thus the extent of conductivity) is controlled by the gate potential, V_G. The current associated with the faradaic processes controlled by V_G is the gate current, I_G. The current that flows between the microelectrodes (when there is a potential difference between them) as a result of the enhanced conductivity of the oxidized $Ni(OH)_2$ film is termed the drain current, I_D. The potential difference maintained between the microelectrodes is the drain voltage, V_D. When V_G equals V_G^1, $Ni(OH)_2$ is reduced (and insulating), and there is no current flowing in the drain circuit, $I_D = 0$. When $Ni(OH)_2$ is oxidized according to equation (1) by moving V_G

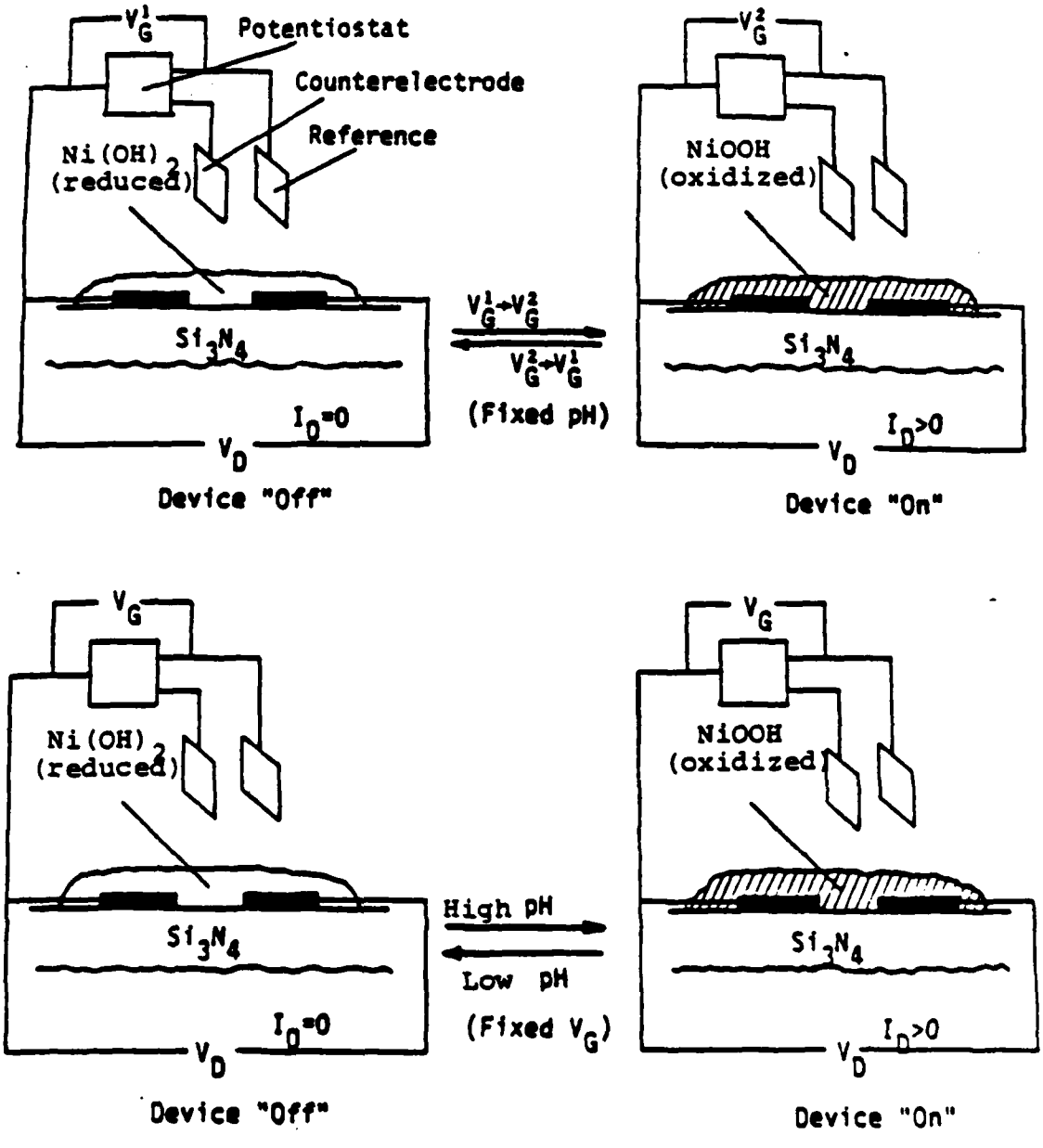

Scheme I. A Ni(OH)$_2$-based transistor that turns on ($I_D > 0$) when V_G is moved from V_G^1 where Ni(OH)$_2$ is reduced and insulating to V_G^2 where Ni(OH)$_2$ is oxidized and conducting. The Ni(OH)$_2$-based device can also be turned on and off by varying the pH at fixed V_G.

to V_G^2, the oxide is conducting, and for a finite V_D, there is current in the drain circuit, $I_D > 0$. The microelectrochemical transistors resemble solid state transistors,[19] but a key difference is that in solid state device I_G is simply a capacitative current, rather than a faradaic current associated with actual electrochemistry.

An important consequence of the faradaic processes occurring in microelectrochemical transistors is that factors which affect the redox chemistry can also affect I_D. The redox potential of $Ni(OH)_2$ is pH-dependent, and therefore I_D is pH-dependent, as illustrated in Scheme I. For a fixed V_G (near the redox potential of $Ni(OH)_2$) and fixed V_D, a change in pH changes the ratio of NiO(OH) to $Ni(OH)_2$, causing a change in I_D. $Ni(OH)_2$-based microelectrochemical transistors can thus function as pH sensors in strongly basic solutions, where the oxide is very durable. Several pH-sensitive microelectrochemical transistors have recently been described,[20] including those based on WO_3,[13] on platinized poly(3-methylthiophene),[21] on ferrocyanide-loaded, protonated poly(4-vinylpyridine),[22] and on a viologen/quinone-based polymer.[23] One important difference between $Ni(OH)_2$ and the other active materials in pH-sensitive transistors is that $Ni(OH)_2$ is especially rugged at pH 14, where none of the other materials can be employed, but it is unstable in acidic media, where the other devices operate.

EXPERIMENTAL SECTION

Preparation of SnO_2 Electrodes. F-doped SnO_2 and In-doped SnO_2 (ITO), used for optical measurements, were obtained from commercial sources. The optical transmittance of F-doped SnO_2 was about 80% in the visible region. Transmittance spectra showed modulations due to optical interference from the SnO_2 film. The sheet resistivity of F-doped SnO_2 was 14 Ω/square as determined by four point probe measurements. F-doped SnO_2 electrodes were cleaned electrochemically prior to $Ni(OH)_2$ deposition by passing anodic, cathodic, and then anodic current at 1 mA/cm^2 for 30 seconds each in 5 M KOH, and In-doped SnO_2 was cleaned by successive sonication in H_2O, isopropanol, and hexane.

Preparation of Microelectrode Arrays. The microelectrodes used in these experiments were of a design previously described.[14-15] Each chip consists of an array of eight parallel Au or Pt microelectrodes on an insulating layer of Si_3N_4, surrounded by macroscopic contact pads. The microelectrodes are 50 μm long, 2.4 μm wide, and 0.1 μm thick, and are separated by 1.2 μm. In some cases, an additional layer of Si_3N_4 was deposited to insulate the entire device except for the actual eight wire array and the contact pads. When Si_3N_4 was not used, the devices were insulated using epoxy. The packaged microelectrode assemblies were then cleaned with an rf O_2 plasma etch (150 W) for 5-8 minutes to remove any residual photoresist or epoxy from the microelectrodes. The microelectrodes were then cycled individually at 200 mV/s 4 or 5 times each from -1.6 to -2.1 V vs. SCE in a 0.05 M pH 7 phosphate buffer. Hydrogen evolution at the negative potential limit further cleans the microelectrodes and ensures reproducible electrochemical behavior. The microelectrodes were then

tested by examining their behavior in an 0.2 M LiCl solution containing 5 mM $Ru(NH_3)_6^{3+}$. A well-defined current-voltage curve at 50 mV/s for the reduction of $Ru(NH_3)_6^{3+}$ is characteristic of a "good" microelectrode.[17]

Reagents. NaOH, KOH, LiOH, CsOH, $NaNO_3$, KNO_3, KH_2PO_4, K_2HPO_4, Na_2CO_3, $NaHCO_3$, and LiCl were used as obtained from commercial sources. $Ru(NH_3)_6Cl_3$ and $Ni(NO_3)_2$ (99.99%) were used as obtained from Alfa. High purity isopropanol and hexane were used. The H_2O used for all experiments was Omnisolv HPLC grade. Unless stated otherwise, all basic solutions contained KOH as the base. None of the solutions were degassed.

Deposition of $Ni(OH)_2$ onto SnO_2 and Microelectrode Arrays. SnO_2 electrodes for transmittance experiments were derivatized with $Ni(OH)_2$ using a literature technique that was optimized.[4a] The electrodes were immersed in 0.01 M $Ni(NO_3)_2$ and cathodic galvanostatic deposition was performed at 0.04 mA/cm^2 for 8 minutes to obtain the desired thickness. Adherent films of $Ni(OH)_2$ were produced. The potential of the working electrode was found to be approximately -0.7 to -0.8 V vs. SCE during the deposition. The thickness of an 8 minute deposition film was measured to be approximately 0.1 μm.

The current densities used for galvanostatic deposition of $Ni(OH)_2$ on SnO_2 were too low to control with accuracy on microelectrode arrays; for this reason, deposition on microelectrodes was performed using potentiostatic control. Adherent films were obtained by holding the potential of the microelectrodes between -0.75 and -0.80 V vs. SCE for 60-100 s in aqueous solutions containing either 0.01 M $Ni(NO_3)_2$, 0.1 M $Ni(NO_3)_2$, 0.1 M $Ni(NO_3)_2$/0.1 M KNO_3, or

0.05 M $Ni(NO_3)_2$/0.05 M $Na(NO_3)$. After an initial spike, the cathodic current decreased during the deposition, indicative of formation of an insulating film of $Ni(OH)_2$ on the microelectrodes. $Ni(OH)_2$ could be deposited selectively onto individual microelectrodes by holding adjacent electrodes, onto which $Ni(OH)_2$ is not deposited, between 0.2 V and 0.3 V vs. SCE. When there was no decrease in the current during the deposition, the electrochemistry of the resulting films was "poor" in that well formed cyclic voltammograms for the $Ni(OH)_2 \rightleftharpoons NiO(OH)$ interconversion could not be detected. In some cases, the deposition procedure was performed twice before electrochemistry of $Ni(OH)_2$ was observed. It has been observed that properties of $Ni(OH)_2$ electrodes are critically dependent upon deposition conditions.[2-6] The conditions used here for microelectrodes typically produce films of $Ni(OH)_2$ approximately 0.5-1.0 μm thick. SnO_2 electrodes used for optical measurements could also be derivatized in this manner.

The electrochemical properties of films prepared using different electrolyte solutions do not vary significantly. With 0.01 M $Ni(NO_3)_2$ as the electrolyte, films of $Ni(OH)_2$ containing both α and β phases are occasionally formed.[24] In such cases the waves collapse to a single peak after repeated cycling. Judging from the location of the redox wave, the α phase is ultimately formed. The best films are obtained when KNO_3 or $NaNO_3$ is added to the electrolyte; sharp single peaks are observed for both oxidation and reduction of the $Ni(OH)_2$ films obtained in such cases.

The derivatized microelectrodes were rinsed in triply distilled H_2O or pH 12 CO_3^{2-}/CO_3H^- buffer, and characterized electrochemically in 1 M KOH.

Equipment. In situ transmittance measurements were obtained with a Bausch and Lomb Spectronic 2000 spectrophotometer. The spectroelectrochemical cell was fashioned from a standard polystyrene cuvette with a 1 cm path length. Time-dependent transmittance at 500 nm was measured using a single beam spectrophotometer with components from Photon Technology International, Inc. and included a Model HH150 high efficiency arc lamp source with a 150 W xenon lamp (Osram) and water filter, monochromator, sample compartment and photomultiplier unit with a 1P28 photomultiplier tube (RCA). Switching measurements were recorded on a Busch Mark 200 strip chart recorder. Time-dependent optical absorbance at 500 nm was measured using a Hewlett-Packard 8451A rapid scan spectrometer. Electrochemical instrumentation consisted of Pine Instruments RDE 4 Bipotentiostats with Kipp and Zonen BD 91 X-Y-Y'-T recorders for microelectrode experiments, and PAR Model 173/175 or Model 273 Potentiostat/Programmers with a Houston Instruments Model 2000 X-Y recorder for SnO_2 experiments. Thickness measurements were made using a Tencor Instruments surface profiler. Flowing streams were produced and delivered to microelectrodes using the pumps of a Hewlett-Packard Model 1084-B liquid chromatograph. Optical micrographs of derivatized microelectrodes were obtained with a Polaroid camera mounted on a Bausch and Lomb MicroZoom optical microscope.

RESULTS AND DISCUSSION

Characterization of Cathodically Deposited $Ni(OH)_2$ on Optically Transparent Electrodes and On Microelectrode Arrays. Thin films of $Ni(OH)_2$ cathodically deposited onto conducting, optically transparent F-doped SnO_2 were characterized by cyclic voltammetry and optical measurements in 1 M KOH. The films were prepared by galvanostatic deposition from solutions of 0.01 M $Ni(NO_3)_2$. The relationship between the cyclic voltammetry and optical transmittance of these films is shown in Figure 1, where the relative transmittance at 500 nm (photomultiplier tube output) is shown along with the cyclic voltammogram obtained at 10 mV/s. The inset to Figure 1 shows the optical spectrum of another $Ni(OH)_2$-coated SnO_2 electrode plotted as % transmittance in the fully reduced and fully oxidized states. As the potential is moved positive, oxidation of $Ni(OH)_2$ to the highly colored NiO(OH) commences, and the relative transmittance declines smoothly. The data indicate that coloration in the visible is essentially complete before all the charge has been withdrawn. A similar phenomenon has been observed for electrochromic WO_3 films[25] which become colored upon reduction to its ultimate extent at less than full reduction. Upon scan reversal, the increase in transmittance is displaced negatively, relative to the decrease found on the forward scan, in correlation with the separation between the location of the anodic and cathodic current peaks.

The cyclic voltammogram for the chemically reversible oxidation of $Ni(OH)_2$ shown in Figure 1 has an interesting shape in two respects. First, the ratio of the anodic to cathodic charge passed on a single

sweep slightly exceeds one. The origin of this phenomenon has recently been investigated in detail, and the results of this study suggest that the excess charge on oxidation is due to oxidation of OH^- in the $Ni(OH)_2$ lattice.[26] The amount of OH^- incorporated in the film can exceed two per $Ni(OH)_2$, meaning that the ratio of anodic charge to cathodic charge can exceed 3:1.[26] At the positive limit there is a small steady state oxidation current corresponding to the evolution of O_2. The second feature of interest in the cyclic voltammogram is that the anodic and cathodic current peak potentials are separated by over 100 mV. This is typically observed for $Ni(OH)_2$ films, regardless of their method of preparation, and is attributed to structural rearrangements required for NiO(OH) reduction.[1-5] The importance of the data in Figure 1 is that the cathodically deposited $Ni(OH)_2$ films behave in a manner consistent with $Ni(OH)_2$ films studied for their electrochromic[6] and battery applications,[1-5] judging from their optical properties and cyclic voltammetry. Thin films of $Ni(OH)_2$ grown on SnO_2 by controlled potential cathodic deposition have properties very similar to those grown by the galvanostatic technique: a displacement is observed in the decoloration of the film corresponding to the location of the cathodic wave of the cyclic voltammogram; the ratio of anodic charge to cathodic charge in the voltammogram is about 2.5:1.

We have characterized the cyclic voltammetry and observed the electrochromic properties of $Ni(OH)_2$ films on microelectrode arrays prepared by controlled-potential cathodic deposition. Consistent with results obtained on SnO_2 electrodes, electrochemical oxidation of the $Ni(OH)_2$-coated microelectrode arrays results in coloration of the

films, as viewed and photographed under an optical microscope. The cyclic voltammetry, at several scan rates, of adjacent Au microelectrodes derivatized with $Ni(OH)_2$ is shown in Figure 2, for a typical controlled-potential deposition. For each of the scan rates, the area of the cyclic voltammogram of both electrodes driven together is essentially the same as those of the individual electrodes. This indicates that there is an electrical connection between the microelectrodes via $Ni(OH)_2$. If there were no connection, the area of the cyclic voltammogram of the two adjacent microelectrodes driven together would be the sum of the individual voltammograms. The cyclic voltammograms in Figure 2 do show some differences, perhaps indicative of sluggish charge transport through the oxide film at the scan rates employed, relative to conducting organic polymers derivatized onto closely spaced microelectrodes.[14-16] Another possibility is that slow proton diffusion might limit the quantity of electroactive material accessible to a microelectrode on the timescale of these experiments.[27] At very slow scan rates, all $Ni(OH)_2$ accessible to one microelectrode is accessible to an adjacent $Ni(OH)_2$-connected microelectrode.

An important property of microelectrode-based transistors is the resistance, as a function of V_G, between two microelectrodes connected by a redox active material. In Figure 3, these data are illustrated for $Ni(OH)_2$-connected microelectrodes at pH 14. Like previously characterized microelectrochemical devices,[13-16] the change in resistance of $Ni(OH)_2$ is associated with injection or withdrawal of charge in an electrochemical redox process. Measurement of the resistance entails bringing adjacent, $Ni(OH)_2$-connected electrodes to

a given V_G, waiting until redox equilibrium is established, and slowly scanning the potential of one microelectrode by a small amount around V_G, while holding the adjacent microelectrode at V_G. With $Ni(OH)_2$-connected microelectrodes, measurements were made 3-5 minutes after moving to a new V_G. Changes in resistance are observed by varying V_G through the region where redox processes occur. The current passing between the electrodes was measured and related to the resistance by Ohm's law. Since the oxidation wave for $Ni(OH)_2$ is particularly sharp, it is important that the potential difference (V_D) developed by scanning one microelectrode is small enough not to seriously affect the ratio of oxidized to reduced material. Thus, typical V_D excursions were ± 3-5 mV.

The data in Figure 3 show that the resistance of $Ni(OH)_2$-connected microelectrodes varies by three orders of magnitude, from ~10^7 ohms to ~10^4 ohms, as V_G is varied from 0.0 to 0.7 V vs. SCE. These data were collected starting at 0 V vs. SCE and moving positive; some hysteresis is observed when measurements are initiated from 0.7 V, in accord with the separation of the oxidation and reduction waves for the $Ni(OH)_2$ film. The measured resistance of different samples may vary from the data in Figure 3 by up to an order of magnitude, but the change in resistance for a particular sample never varies by more than four orders of magnitude. The resistance of $Ni(OH)_2$-connected microelectrodes in the oxidized, conducting state is much higher than for reduced WO_3[13] or oxidized conducting organic polymers[14-16] derivatized on microelectrodes. In the insulating state, the resistance, as for WO_3,[13] is lower than for the conducting organic polymers.[14-16] The low resistance of this semiconducting oxide in the

"insulating" state may be a consequence of the high concentration of doping impurities in solution.

A manifestation of the sharpness of the oxidation wave for $Ni(OH)_2$, compared to other redox active conducting materials, is the slope of the resistance-V_G plot in Figure 3. Nearly the entire three order of magnitude change in resistance occurs between V_G = 0.3 and 0.4 V vs. SCE, the sharpest change in resistance found to date for any conducting material derivatized onto microelectrodes. The resistance of $Ni(OH)_2$-connected microelectrodes per se is not an especially meaningful parameter, since it can only be referenced to the resistance of other redox active electronic conductors derivatized on closely spaced microelectrodes of the same geometry. Unlike the resistance, R, the resistivity, ρ, defined in equation (2), is a characteristic property of a material.

$$R = \rho (l/A) \qquad (2)$$

In equation (2), l is the length of a uniform conductor, and A is its cross sectional area. Assuming complete uniformity of oxidized $Ni(OH)_2$ films, an approximate calculation of the resistivity can be made using the well-defined microelectrode geometry. For typical $Ni(OH)_2$-based devices, the 50 μm long microelectrodes are covered with a 0.5-1.0 μm thick film. The length is taken to be the 1.2 μm spacing between microelectrodes. Calculations reveal that in the conducting state, the resistivity of cathodically deposited $Ni(OH)_2$ is 20-40 Ω-cm. This value is five or six orders of magnitude higher than for elemental metals, and about equal to the resistivity of highly doped

single crystal semiconductors. The sample to sample variability in resistance is probably a result of differences in film thickness rather than in resistivity. While the resistivity of $Ni(OH)_2$ may be high for a "conducting" material, it is the potential dependence of the resistivity that leads to interesting consequences.

Transistor Properties of $Ni(OH)_2$-Connected Microelectrodes. It has been established that materials that undergo large changes in resistance can exhibit transistor-like behavior when derivatized on closely spaced microelectrode arrays.[13-16,20-23] We have characterized the transistor properties of $Ni(OH)_2$-connected microelectrodes, and as expected from the relatively slow charge transport and the relatively high resistance of the conducting state, the response times and amplification properties of the films are not comparable to those of conducting materials such as poly(3-methyl)thiophene and polyaniline, that can amplify power at frequencies approacning 1 kHz.[28] Nevertheless, the $Ni(OH)_2$-based devices function at high pH, a regime where none of the other conducting materials on microelectrodes characterized to date are durable.

Scheme I shows that when V_G is moved from V_G^1, where $Ni(OH)_2$ is reduced, to V_G^2, where $Ni(OH)_2$ is oxidized, and there is a potential difference (V_D) between two adjacent microelectrodes, I_D can be expected to go from zero to a finite value that depends on the magnitude of V_D. Figure 4 shows I_D versus time when a $Ni(OH)_2$-based transistor is stepped from a V_G of 0.1 to 0.45 V vs. SCE and back. With V_D = 100 mV, I_D shifts reproducibly from zero at V_G = 0.1 V vs. SCE to 150 μA at V_G = 0.45 V vs. SCE. The limiting I_D for the 100 mV

V_D implies a resistance of approximately 6 X 10^5 ohms at 0.45 V vs. SCE, meaning that this device is more resistive than the one characterized in Figure 3. The device takes approximately 20 seconds to achieve a steady state I_D with a 100 mV V_D but achieves >80 % of its maximum I_D in <2 s. The current spikes upon scan reversal are indicative of the charging current necessary to turn the device on and off. While the magnitude of I_D is limited at fixed V_D by the resistance and therefore, V_G, the rate at which a particular I_D is attained is determined by rate of faradaic processes in the gate circuit. Electron motion within the oxide is not thought to be limiting in the electrochemistry of $Ni(OH)_2$ films. Rather, slow diffusion of protons in and out of the films limits the rate of charge transport.[27] The proton diffusion coefficient, D_H, during oxidation and reduction has been found to be 3.1 x 10^{-10} cm^2/s and 4.6 x 10^{-11} cm^2/s, respectively.[27] Surprisingly, upon stepping to 0.1 V vs. SCE, I_D returns to zero in less than 2 seconds, although D_H for reduction is smaller than for oxidation. However, charging and discharging are not symmetric processes, and this behavior has been noted with other oxides. For example, reduction of WO_3 films is faster than oxidation of H_xWO_3.[25] We have obtained reproducible I_D- V_G characteristics during the course of the characterization, a period of about one hour.

Evidence that $Ni(OH)_2$-based microelectrochemical transistors function as electrical power amplifiers is illustrated in Figure 5, which shows the magnitudes and relationships of V_G, I_G, and I_D, for a slow triangular potential variation between 0 V and 0.45 V vs. SCE. In these experiments, three adjacent, $Ni(OH)_2$-connected microelectrodes are used; I_G is recorded for the center

microelectrode, while I_D is recorded for a separate circuit between the outer "source" and "drain" microelectrodes. While these relationships are best understood with respect to a sinusoidally varying V_G, they can be interpreted with a triangular V_G as well. In principle, I_G and I_D should equal zero at V_G = 0 V vs. SCE because $Ni(OH)_2$ is reduced and insulating at this V_G. As V_G is scanned positive, anodic I_G is observed until all the material in the gate region has been oxidized. When V_G reaches its upper limit, I_G should once again be zero. Upon scan reversal, the reverse electrochemical process is a reduction. I_D should equal zero until enough charge is withdrawn from $Ni(OH)_2$ in the gate circuit to turn on the device, and should return to zero when sufficient charge is injected to turn off the device. The data in Figure 5, for a V_G frequency of 3.8×10^{-2} Hz, nearly obeys the relationships outlined above. The integrated I_G is greater for oxidation than for reduction, due to the oxidation of excess OH^- in the lattice, and this may contribute to the non-ideal relationship between I_G and V_G. I_D behaves as expected at this 3.8×10^{-2} Hz, following the variation in V_G in a manner consistent with data in Figure 3. It is important to note that I_G does not go to zero if V_G is held at the positive limit, because OH^- is oxidized. In all other microelectrochemical transistors [13-17,20] I_G does become negligible under such conditions.

The average power amplification, A, is given by equation (3).

$$A = \frac{\text{average power in the drain circuit}}{\text{average power in the gate circuit}} \qquad (3)$$

For the data shown in Figure 5, A is equal to 2. In calculating A, we

have used the cathodic portion of the cyclic voltammogram as an indication of I_G, due to the extra charge in the anodic wave. The maximum amplification we have observed is approximately 20. This number should be compared to power amplification (at low frequency,<1 Hz) of approximately 10^4 for devices from poly(3-methylthiophene) and polyaniline,[28] and about 200 for WO_3-based transistors.[13] In theory, at the same frequency and surface coverage, differences between microelectrochemical transistors in the ability to amplify electrical power depend on the maximum conductivity of the materials used to connect adjacent microelectrodes. The observed amplification properties for devices prepared from $Ni(OH)_2$, WO_3, and the conducting organic polymers accurately reflect the relative maximum conductivities of the materials. Power amplification is frequency-dependent in that I_G increases with scan rate. Furthermore, at sufficiently high frequencies, limitations in rates of faradaic processes preclude complete turn on/turn off. The data in Figure 5 are obtained in the mHz frequency domain, while polyaniline-based microelectrochemical transistors can amplify electrical power at frequencies approaching 1 kHz.[28] The slow operating speed of $Ni(OH)_2$-based microelectrochemical transistors is limited by the slow electrochemistry of the $Ni(OH)_2$ films. At frequencies higher than ~1 mHz, $Ni(OH)_2$-based transistors do not amplify power, since $\underline{A} < 1$.

There are several ways to increase the power gain and operating frequencies of $Ni(OH)_2$-based transistors. The most straightforward approach is to prepare films with lower resistance in the conducting state. However, even if this is not possible, the geometry of $Ni(OH)_2$-based microelectrochemical transistors can be modified so as

to increase the net amplification. For instance, the spacing between microelectrodes can be closed.[20] By equation (2), we could expect the measured resistance to decrease linearly with the distance between adjacent microelectrodes, since the dimension l is reduced. In addition, the volume of oxide needed to connect microelectrodes would be reduced by closing the gap, which yields the added benefit of reducing the charge involved in oxidizing $Ni(OH)_2$. Insulating the tops of microelectrode wires, so that only the side walls of the microelectrodes are exposed, would further reduce the volume of electroactive material needed to make an electrical contact.[28] Work along these lines is in progress.

Even when there is no power amplification, useful information can be obtained by simultaneously monitoring I_G and I_D as V_G is varied. We wished to know to what extent the increase in conductivity is correlated to charge injection in $Ni(OH)_2$ films, and whether the extra anodic charge, Q_a, associated with OH^- oxidation has any effect on the bulk conductivity of $Ni(OH)_2$. Data pertaining to these issues are shown in Figure 6, which shows the relationship between integrated cathodic charge, Q_c, integrated anodic charge, Q_a, and I_D for $Ni(OH)_2$-based transistors at pH 14, as a function of V_G. Q_c represents the charge associated with the reversible $NiO(OH)/Ni(OH)_2$ redox reaction. Q_a includes Q_c plus the extra, irreversible charge associated with OH^- oxidation.[26] Because of the slow response of these films, I_D generally increased with time. To compensate for this, scan rates were varied with the potential limits so that varying amounts of charge were injected and withdrawn in the same amount of time. For example, potential sweeps from 0 V to 0.50 V vs. SCE were performed at

50 mV/s, to 0.60 V vs. SCE at 60 mV/s, etc. Under these conditions, valid comparisons fo I_D, Q_c, and Q_a can be made. The data plotted in Figure 6 are averages of several measurements. As the positive scan limit is increased, Q_c increases and levels off; on the other hand, Q_a increases monotonically. This data is collected from the V_G regime where oxidation of the film is essentially complete, judging from the levelling in Q_c. I_D roughly follows the shape of the Q_c curve, indicating correspondence between charge associated with NiO(OH) reduction and I_D. At 0.375 V vs. SCE and lower values of V_G, I_D deviates from the Q_c curve because of leakage current in the drain circuit at the scan rates employed. At values of V_G exceeding 0.55 V vs. SCE, I_D and Q_c increase only slightly. In contrast, at these potentials very large increases in Q_a are recorded, due to bulk O_2 evolution. These data indicate that any excess Q_a passed that is not a result of the oxidation of $Ni(OH)_2$ films has no bearing on the conductivity of the film. Furthermore, this data shows that at values of V_G where charge withdrawal does not lead to increased visible coloration (Cf. Figure 1), it still leads to increased conductivity.

As a final characterization of $Ni(OH)_2$-based transistors, we have measured the temperature dependence of I_D. The Arrhenius form of the temperature dependence of I_D is shown in equation (4), where I_D^o represents a collection of constants, R is the gas constant, T is

$$I_D = I_D^o \exp[-E_a/RT] \qquad (4)$$

temperature in degrees Kelvin, and E_a is the activation energy for conductivity. E_a should not depend on V_G, since $[NiO(OH)]/[Ni(OH)_2]$

is fixed at a given V_G. Figure 7 shows the temperature dependence of I_D for a $Ni(OH)_2$-based transistor at pH 14, with V_G = 0.35 V vs. SCE, and V_D = 0.1 V. I_D is plotted on a logarithmic scale vs. T^{-1} . A reasonably large temperature dependence is found; the energy of activation for charge transport is calculated from the slope of the best-fit line and found to be 27 ± 2 kJ/mol, at V_G = 0.35 V vs. SCE. It is possible that a temperature dependence of the $Ni(OH)_2$ redox potential could alter the ratio $[NiO(OH)]/[Ni(OH)_2]$, especially at potentials where the conductivity is sensitive to V_G. However, the temperature dependence of the redox potential was found to be negligible by cyclic voltammetry in the temperature range investigated. Furthermore, determination of E_a for a different sample at V_G = 0.45 V vs. SCE and V_D = 50 mV, where $Ni(OH)_2$ is completely oxidized, gave a value of 23 ± 2 kJ/mol. Thus, we are confident that the temperature dependence of I_D is related to the activation energy for conductivity. Temperature-dependent conductivities have been reported in the dry state for polyacetylene,[29] polyaniline,[30] polypyrrole,[31] poly(3-methylthiophene),[32] polythiophene[33] and NiO.[34] All of the systems in their conducting state, except NiO[34], show a small temperature dependence of conductivity compared to the $NiO(OH)/Ni(OH)_2$ system. In the case of polythiophene, for example, the activation energy of conductivity decreases, from 77 kJ/mol in the neutral (essentially insulating) state to 3 kJ/mol for a heavily doped (conducting) sample, upon electrochemical doping.[33] The concept of shallow and deep polaron and bipolaron[33,35] is used to explain the temperature dependence of conductivity for neutral and doped polythiophene. At heavy doping levels, a hole conduction mechanism is

suggested and characterized by a small activation energy.[33] The activation energy of conductivity found in the present study (~25 kJ/mol) for $NiO(OH)/Ni(OH)_2$ is in agreement with previously reported values (29-77 kJ/mol) for NiO in the dry state.[34] It also resembles activation energies (20-50 kJ/mol) found for conventional redox polymer "conductors".[22,36] In NiO and others 3d transition metal oxides, electrons in the incomplete 3d shell are thought to be localized due to strong electron-electron correlation and the carrier transport is thermally activated as expected in hopping conduction[34] and in redox conductivity.[22,36]

pH Dependence of $Ni(OH)_2$-Based Transistors. The pH dependence of $Ni(OH)_2$ redox electrochemistry is well documented.[37] Since the redox properties of $Ni(OH)_2$ modulate its conductivity, the resulting transistor properties are also pH-dependent. The left side of Figure 8 shows the cyclic voltammograms for $Ni(OH)_2$-connected microelectrodes at three different pH's. The pH dependence is demonstrated by the shift in the redox potential of the voltammetric wave associated with the $Ni(OH)_2$ oxidation. Interestingly, Q_c changes with pH as well, indicating that in strongly basic solution more $Ni(OH)_2$ is electrochemically accessible. This may be a consequence of structural changes caused by variation in pH. This phenomenon is reversible down to pH 10; at lower pH electrochemical oxidation of $Ni(OH)_2$ is not observed, probably due to irreversible degradation of the film. It is also possible that at low pH's, $Ni(OH)_2$ is not firmly bound to the microelectrode surface. The right side of Figure 8 shows V_D-I_D plots for $Ni(OH)_2$-based transistors for several values of V_G, at the same pH as for the cyclic voltammograms. The V_G at which the transistor turns

on is signified by non-zero I_D as V_D is scanned. For instance, at pH 13.7, the device is off at V_G = 0.30 V vs. SCE, and begins to turn on at 0.31 V vs. SCE. Significantly, the turn-on potential varies with the onset of the cyclic voltammetric wave as the pH is varied, confirming that electrochemical oxidation of $Ni(OH)_2$ is responsible for the increase in conductivity.

The effect of pH on the I_D-V_G characteristics of the transistor (at fixed V_D) is further illustrated by the data in Figure 9, that shows steady state I_D at V_D = 50 mV as a function of V_G for $Ni(OH)_2$-based microelectrochemical transistors, at five different pH's. As the pH is lowered, the maximum value of I_D steadily decreases. In addition, the shift in the turn-on V_G with pH is illustrated. This data shows how a pH-sensitive $Ni(OH)_2$-based microelectrochemcial transistor might operate: at fixed V_G and V_D, a change in pH gives rise to a change in I_D, as shown in Scheme I. It is important to point out that the pH regime in which a $Ni(OH)_2$-based device could operate is restricted to values of pH where reversible electrochemistry for $Ni(OH)_2$ is obtained, namely pH $\geq$ 10. However, none of the pH-sensitive microelectrode-based chemical transistors developed to date can operate at high pH.[13,20-23] One way to evaluate the I_D-V_G characteristic is to calculate the maximum slope of the plots, which is closely related to the "transconductance" of solid state transistors.[19] The maximum slope of the I_D-V_G plot is 6 μA/V. The comparable number for poly(3-methylthiophene)-based devices is 6 mA/V, three orders of magnitude greater. In spite of the steepness of the resistance-V_G for $Ni(OH)_2$, the higher overall conductivity of poly(3-methylthiophene) gives rise to higher changes in I_D per unit

change in V_G. It should be noted that the small maximum slope of the I_D-V_G plot for $Ni(OH)_2$-based devices is not a hurdle to operation as a chemically sensitive transistor, since the I_D output can always be further amplified. Finally, regarding the pH dependence of the $Ni(OH)_2$, note that Figures 8 and 9 show that lower pH's give higher resistivity. This higher resistivity correlates with decreased Q_a and Q_c associated with the $Ni(OH)_2 \rightleftharpoons NiO(OH)$ interconversion.

A potential obstacle to the use of $Ni(OH)_2$-based devices as pH sensors is interfering cations. It is known that Na^+ and Li^+ can intercalate into several electrochromic transition metal oxides.[7] We find that the cyclic voltammetry of $Ni(OH)_2$-connected microelectrodes is independent of the choice of cation (1 M Li^+, Na^+ and K^+) for OH^- at pH 14, and further, there is no difference in the value of I_D for $Ni(OH)_2$-based transistors exposed to these different media. There are reports of K^+ insertion into NiO(OH),[2,3] but we find no consequence with respect to transistor characteristics. It should be noted as well that we have found no evidence at any pH for cation interference in WO_3-based device,[13] although WO_3 is known to intercalate Li^+, Ag^+, and Na^+.[8]

Figure 10 shows I_D over time for a $Ni(OH)_2$-based microelectrochemical transistor as the pH of a stream flowing past the microelectrode array is reproducibly varied between pH 12 and pH 13. With V_G = 0.35 V vs. SCE, and V_D =50 mV, the composition of the stream flowing at the rate of 4.0 ml/min is changed from 100% pH 12 0.05 M Na_2SO_4 to 100% pH 13 0.05 M Na_2SO_4. I_D changes from ~1 μA at pH 12 to ~3.5 μA at pH 13. The change in pH, accomplished by switching solvent pumps of an HPLC, takes approximately one minute at this flow rate.

The response time of the device is fast enough to follow the pH variation. There is a small, but noticeable, drift in I_D at pH 12, indicating that the device is not turning off fully. In fact, from the data in Figure 10, one might expect to see $I_D = 0$ at pH 12 under these conditions. However, for this device, the long term steady state value for I_D is -1 μA, measured by maintaining a pH 12 stream indefinitely. At this pH, when V_G is moved to 0.30 V vs. SCE, $I_D \approx 0$. At pH 13, with V_G = 0.30 V vs. SCE, $I_D \approx 3$ μA. For this particular device, the I_D-V_G curves of Figure 10 are displaced to slightly lower potentials. The response was reproducible through the course of the 6 h experiment. The cyclic voltammetry of the $Ni(OH)_2$-derivatized microelectrodes the following day was identical to that recorded prior to the experiment. At high pH, $Ni(OH)_2$-based transistors are quite rugged. The long term durability of $Ni(OH)_2$ in basic solution is one reason for its utility as a rechargeable battery material.[1-5] The important point from the data in Figure 10 is that $Ni(OH)_2$-based transistors can reproducibly sense small changes in pH and can give fairly reproducible response under actual operating conditions. The sharpness of the redox wave which modulates $Ni(OH)_2$ conductivity, illustrated by the data in Figures 2 and 3, indicates that it might be possible to sense much smaller changes in pH in basic solutions.

CONCLUSIONS

The operation of pH-sensitive microelectrochemical transistors based on cathodically deposited $Ni(OH)_2$ has been demonstrated. The $Ni(OH)_2$ on microelectrodes behaves in a similar manner to $Ni(OH)_2$ used in electrochromic and rechargable battery applications. The cathodically deposited films connect adjacent microelectrodes allowing

the resistance of $Ni(OH)_2$ as a function of potential to be measured. The resistance of $Ni(OH)_2$-connected microelectrodes decreases by over three orders of magnitude upon electrochemical oxidation.

$Ni(OH)_2$-based microelectrochemical transistors are poor power amplifiers compared to previously characterized conducting materials, and furthermore, response time is slow due to sluggishness of $Ni(OH)_2$ redox electrochemistry. The prospect of substantial improvements in both amplification and response time are realistic possibilities based on improved microelectrode design and increased diffusion coefficients for protons. Simultaneous measurement of I_G, I_D, and V_G allows the conclusion that excess anodic charge in the cyclic voltammetry of $Ni(OH)_2$, a consequence of OH^- oxidation, has no effect on the conductivity of the material. The integrated cathodic charge, which corresponds to the charge involved in $Ni(OH)_2 \rightleftharpoons NiO(OH)$ interconversion, correlates well with I_D. However it should be emphasized that $I_G \neq 0$ when a $Ni(OH)_2$-based transistor is held in the "on" state. Though the steady state value of I_D is always much greater than I_G, this "leakage" current is much greater than in solid state transistors[19] or other microelectrochemical transistors.[13-17,20]

pH-dependent transistor properties observed are in agreement with predictions based on the pH-dependence of the electrochemical oxidation of $Ni(OH)_2$. The useful pH regime has been demonstrated to be 10 to 14. $Ni(OH)_2$-based microelectrochemical transistors are able to reproducibly respond to a change from pH 12 to 13 in a flowing stream for period exdeeding 6 h. The response time is adequate for sensors applications and the durability of such devices in basic solutions is impressive.

Acknowledgements. We thank the Office of Naval Research and the Defense Advanced Research Projects Agency for partial support of this research at M.I.T.. We thank D. A. Corrigan for helpful discussions and R.A. Conell for assistance with optical measurements. Daniel Bélanger also acknowledges le Fonds pour la Formation de Chercheurs et l'Aide à la Recherche of Québec for partial support as a postdoctoral fellow, 1986.

References

1. Gunther, R. and Gross, S. eds., "Proceedings of the Symposium on the Nickel Electrode", The Electrochemical Society, Battery Division, Vol. 82-84, 1984.

2. (a) Halpert, G. J. Power Sources, 1984, 12, 177; (b) Olivia, P.; Leonaredi, J.; Laurent, J. F. J. Power Sources, 1982, 8, 229; (c) Barnard, R.; Randell, C. F.; Tye, F. L. J. Appl. Electrochem., 1980, 10, 109; (d) Barnard, R.; Randell, C. F.; Tye, F. L. J. Appl. Electrochem., 1980, 10, 127.

3. (a) MacDougall, B.; Graham, M. J. J. Electrochem. Soc., 1981, 128, 2321; (b) Wilhelm, S. M.; Hackerman, N. J. Electrochem. Soc., 1981, 128, 1668; (c) Glarum, S. H.; Marshall, J. H. J. Electrochem. Soc., 1982, 129, 535; (d) Schrebler Guzman, R. S.; Vilche, J. R.; Arvia, A. J. J. Appl. Electrochem., 1979, 9, 183; (e) Schrebler Guzman, R. S.; Vilche, J. R.; Arvia, A. J. J. Appl. Electrochem., 1979, 9, 321; (f) Schrebler Guzman, R. S.; Vilche, J. R.; Arvia, A. J. J. Electrochem. Soc., 1978, 128, 1578.

4. (a) Falk, S. U. and Salkind, A. J. Eds., "Alkaline Storage Batteries", John Wiley and Sons: New York, 1969; (b) McEwen, R. S. J. Phys. Chem., 1971, 75, 1782; (c) Briggs, G. W. D.; Wynne-Jones, W. F. K. Electrochim. Acta, 1962, 7, 241.

5. (a) Tuomi, D. J. Electrochem. Soc., 1965, 112, 1; (b) Manandhar, K.; Pletcher, D. J. Appl. Electrochem., 1979, 9, 707; (c) Tench, D.; Warren, L. F. J. Electrochem. Soc., 1983, 130, 869.

6. (a) McIntyre, J. D. E.; Peak, W. F.; Schwartz, G. P. 21st Electronic Materials Conference (Boulder, CO, USA, 1979), Paper D4; (b) McIntyre, J. D. E. 22nd Electronic Materials Conference (Cornell, NY, USA, 1980), paper A1; (c) Lampert, C. M.; Omstead, T. R.; Yu, T. C. in "Proceedings of S.P.I.E.-International Society of Optical Engineering", Lampert, C. M., Ed., Vol. 562, S. P. I. E.: Bellingham, WA, 1985, p. 15.

7. (a) Dautremont-Smith, W. C. Displays, 1982, 3, 3; (b) Dautremont-Smith, W. C. Displays, 1982, 3, 67; (c) Agnihotry, S. A.; Saini, K. K.; Subhas Chandra Ind. J. of Pure and Appl. Phys., 1986, 24, 19.

8. (a) Deb, S. K. Philos. Mag., 1973, 27, 807; (b) Faughnan, B. W.; Crandall, R. S.; Lampert, M. A. Appl. Phys. Lett., 1975, 27, 275; (c) Hersh, H. N.; Kramer, W. E.; McGee, J. H. Appl. Phys. Lett., 1975, 27, 646.

9. (a) Dyer, C. K.; Leach, J. S. J. Electrochem. Soc., 1978, 125, 23; (b) Reichman, B.; Bard. A. J. J. Electrochem. Soc., 1980, 127, 241.

10. (a) Buckley, D. N.; Burke, L. D. J. Chem. Soc. Faraday Trans. I., 1975, 71, 1447; (b) Gottesfeld, S.; McIntyre, J. D. E.; Beni, G.; Shay, J. L. Appl. Phys. Lett., 1978, 33, 208.

11. (a) Arnoldussen, T. C. J. Electrochem. Soc., 1976, 123, 527; (b) Rabelais, J. W.; Colton, R. J.; Guzman, A. M. Chem. Phys. Lett., 1974, 29, 131; (c) Colton, R. J.; Guzman, A. M.; Rabelais, J. W. J. Appl. Phys., 1978, 49, 409; (d) Dickens, P. G.; Birtill, J. J. J. Electron. Mat., 1978, 7, 679.

12. (a) Gottesfeld, S. J. Electrochem. Soc., 1980, 127, 272; (b) Burke, L. D.; O'Sullivan, E. J. M. J. Electroanal. Chem., 1978, 93, 11.

13. (a) Natan, M. J.; Mallouk, T. E.; Wrighton, M. S. J. Phys. Chem. in press; (b) Natan, M. J. Ph.D. Thesis, Massachusetts Institute of Technology, Cambridge, MA, 1986.

14. (a) White, H. S.; Kittlesen, G. P; Wrighton, M. S. J. Am. Chem. Soc., 1984, 106, 5375; (b) Kittlesen, G. P; White, H. S.; Wrighton, M. S. J. Am. Chem. Soc., 1984, 106, 7389; (c) Kittlesen, G. P. Ph.D. Thesis, Massachusetts Institute of Technology, Cambridge, MA, 1985.

15. Paul, E. W.; Ricco, A. J.; Wrighton, M. S. J. Phys. Chem., 1985, 89, 1441.

16. (a) Thackeray, J. W.; White, H. S.; Wrighton, M. S. J. Phys. Chem., 1985, 89, 5133; (b) Thackeray, J. W. Ph.D. Thesis, Massachusetts Institute of Technology, Cambridge, MA, 1986.

17. (a) Kittlesen, G. P.; White, H. S.; Wrighton, M. S. J. Am. Chem. Soc., 1985, 107, 7373; (b) Kittlesen, G. P.; Wrighton, M. S. J. Mol. Electronics, 1986, 2, 23.

18. Leventis, N.; Natan, M. J.; Schloh, M. O.; Wrighton, M. S. unpublished results.

19. Sze, S. M. "Physics of Semiconductor Devices"; Wiley: New York, 1981.

20. Wrighton, M. S.; Thackeray, J. W.; Natan, M. J.; Smith, D. K.; Lane, G. A.; Bélanger, D. Phil. Trans. Roy. Soc. Ser. B, in press.

21. Thackeray, J. W.; Wrighton, M. S. J. Phys. Chem., 1986, 90, 0000.

22. Bélanger, D.; Wrighton, M. S. submitted to Anal. Chem.

23. (a) Smith, D. K.; Lane, G. A.; Wrighton, M. S. J. Am. Chem. Soc., 1986, 108, 3522; (b) Smith, D. K.; Lane, G. A.; Wrighton, M. S. in preparation.

24. (a) Bode, H.; Dehmelt, K.; Nitte, J. Electrochim. Acta, 1966, 11, 1074.

25. Faughnan, B. W.; Crandall, R. S. in "Topics in Applied Physics", Pankove, J. I., ed., Vol. 40, Springer-Verlag: Berlin, 1980.

26. Carbonio, R. E.; Macagno, V. A.; Arvia, A. J. J. Electroanal. Chem., 1984, 177, 217.

27. MacArthur, D. M. J. Electrochem. Soc., 1970, 117, 729.

28. Lofton, E. P.; Thackeray, J. W.; Wrighton, M. S. J. Phys. Chem., 1986, 90, 6080.

29. Chiang, C. K.; Fincher, C. R., Jr.; Park, Y. W.; Hegger, A. J.; Shirakawa, H.; Louis, E. J.; Gau, S. C.; MacDiarmid, A. G.; Phys. Rev. Lett., 1977, 39, 1098.

30. Langer, J. Solid State Commun., 1978, 26, 839.

31. Kanazawa, K. K.; Diaz, A. F.; Gill, W. D.; Grant, P. M.; Street, G. B.; Gardini, G. P.; Kwak, J. F. Synth. Met., 1980, 1, 329.

32. Hotta, S.; Hosaka, T.; Shimotsuma, W.; Synth. Met., 1983, 6, 317.

33. Kaneto, K.; Hayashi, S.; Ura, S.; Yoshino, K. J. Phys. Soc. Jpn., 1985, 54, 1146.

34. Goodenough, J. B. Progr. Solid State Chem., 1971, 5, 145.

35. (a) Scott, J. C.; Pfluger, P.; Krounbi, M. T.; Street, G. B. Phys. Rev. B, 1984, 28, 2140.; (b) Brédas, J. L.; Scott, J. C.; Yakushi, K.; Street, G. B. Phys. Rev. B, 1984, 30, 1023.

36. (a) Oyama, N.; Anson, F.C. J. Electrochem. Soc., 1980, ,127,640; (b) Oyama, N.; Ohsaka, T.; Ushirogouchi, T. J. Phys. Chem., 1984, 88, 5274.

37. (a) McArthur, D. M. J. Electrochem. Soc., 1970, 117, 422; (b) Barnard, R.; Randell, C. F.; Tye, F. L. J. Appl. Electrochem., 1981, 11, 517; (c) Burke, L. D.; Twomey, T. A. M. J. Electroanal. Chem., 1982, 134, 353;

Figure Captions

Figure 1. Simultaneous measurement of the cyclic voltammetry (10 mV/s) and relative transmittance at 500 nm of a 0.1 μm thick film of $Ni(OH)_2$ deposited cathodically on transparent, conducting, F-doped SnO_2, at pH 14. The inset shows % transmittance of the fully reduced and fully oxidized film.

Figure 2. Cyclic voltammograms at pH 14 of individual adjacent $Ni(OH)_2$-connected microelectrodes and of the pair driven together, at several scan rates.

Figure 3. Resistance of $Ni(OH)_2$-connected microelectrodes as a function of V_G at pH 14. The data was obtained by scanning one microelectrode ±5 mV about V_G at 2 mV/sec; V_G was moved anodically. The resistance is plotted on a logarithmic scale.

Figure 4. I_D vs. time for a $Ni(OH)_2$-based transistor at pH 14 as V_G is stepped repetitively every 20 s from 0.1 to 0.45 V vs. SCE and back. V_D = 100 mV.

Figure 5. Simultaneous measurement and phase relationship of V_G, I_G, and I_D for a $Ni(OH)_2$-based microelectrochemical transistor at pH 14 as V_G is repetitively swept linearly from 0.1 to 0.425 V vs. SCE and back at a frequency of 3.8×10^{-2} Hz. V_D = 200 mV.

Figure 6. I_D, cathodic charge (Q_c), and anodic charge (Q_a) for a $Ni(OH)_2$-based microelectrochemical transistor vs. V_G for cyclic voltammograms from 0 V vs. SCE to V_G. The scan rate was varied so that the time required to complete a single cycle was 20 seconds. pH = 14. V_D = 50 mV.

Figure 7. I_D vs. temperature^{-1} at pH 14 for a $Ni(OH)_2$-based microelectrochemical transistor, with V_G = 0.35 V vs. SCE, and V_D = 100 mV. I_D is plotted on a logarithmic scale.

Figure 8. pH dependence of the cyclic voltammetry and I_D-V_D plots (for several V_G's) for a $Ni(OH)_2$-based microelectrochemical transistor. The scan rate for the cyclic voltammograms was 50 mV/sec, and for the I_D-V_D plots was 10 mV/s.

Figure 9. pH dependence of steady state I_D vs. V_G (at fixed V_D = 50 mV) for a $Ni(OH)_2$-based microelectrochemical transistor.

Figure 10. I_D vs. time for a $Ni(OH)_2$-based microelectrochemical transistor as the pH of a continuously flowing stream is varied from 12 to 13. V_G = 0.35 V vs. SCE and V_D = 50 mV.

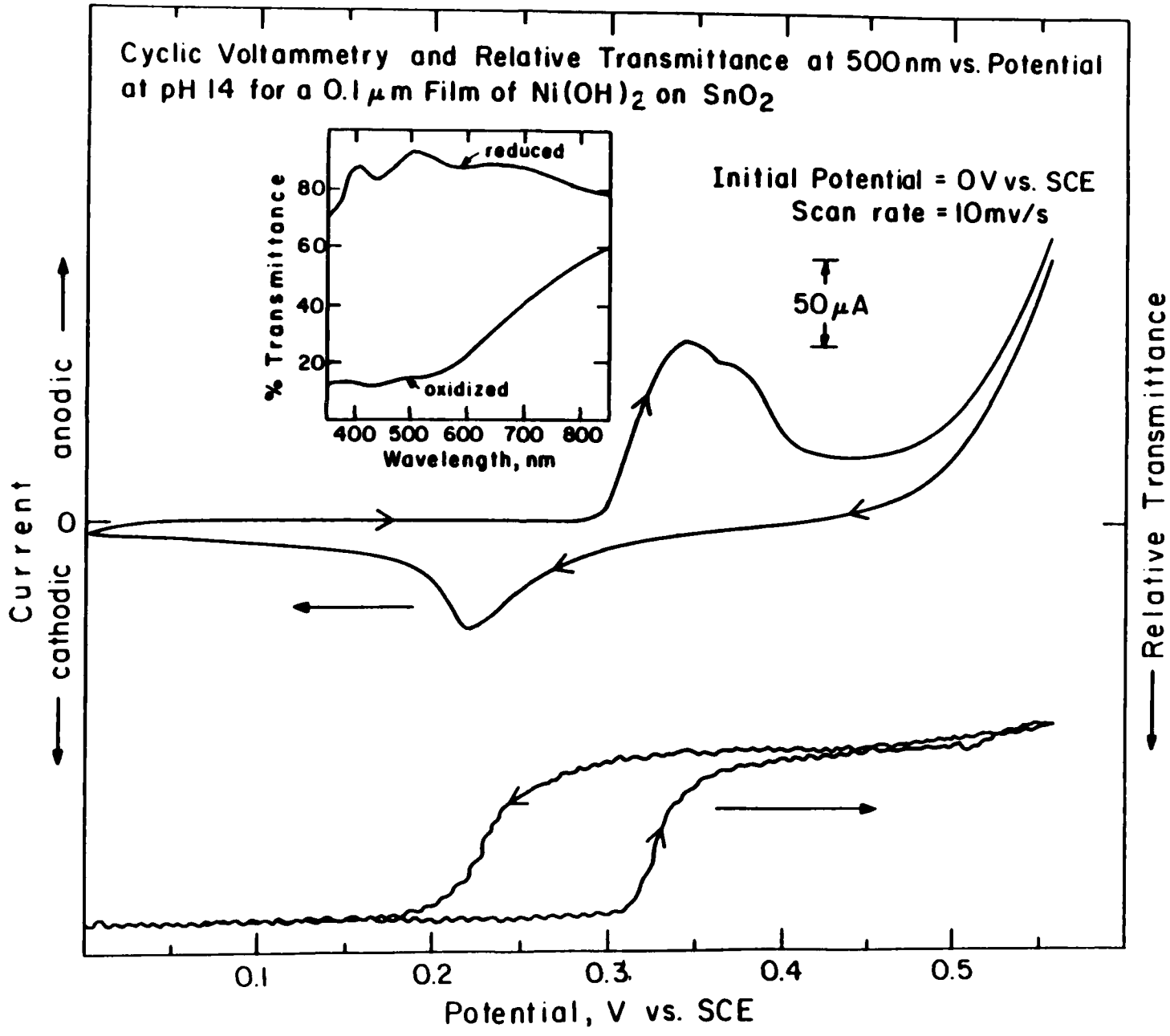
Cyclic Voltammetry and Relative Transmittance at 500nm vs. Potential at pH 14 for a 0.1 μm Film of Ni(OH)2 on SnO2
reduced
oxidized
% Transmittance
80
60
40
20
400 500 600 700 800
Wavelength, nm
Initial Potential = 0V vs. SCE
Scan rate = 10mv/s
50μA
Current
cathodic 0 anodic
Relative Transmittance
0.1
0.2
0.3
0.4
0.5
Potential, V vs. SCE

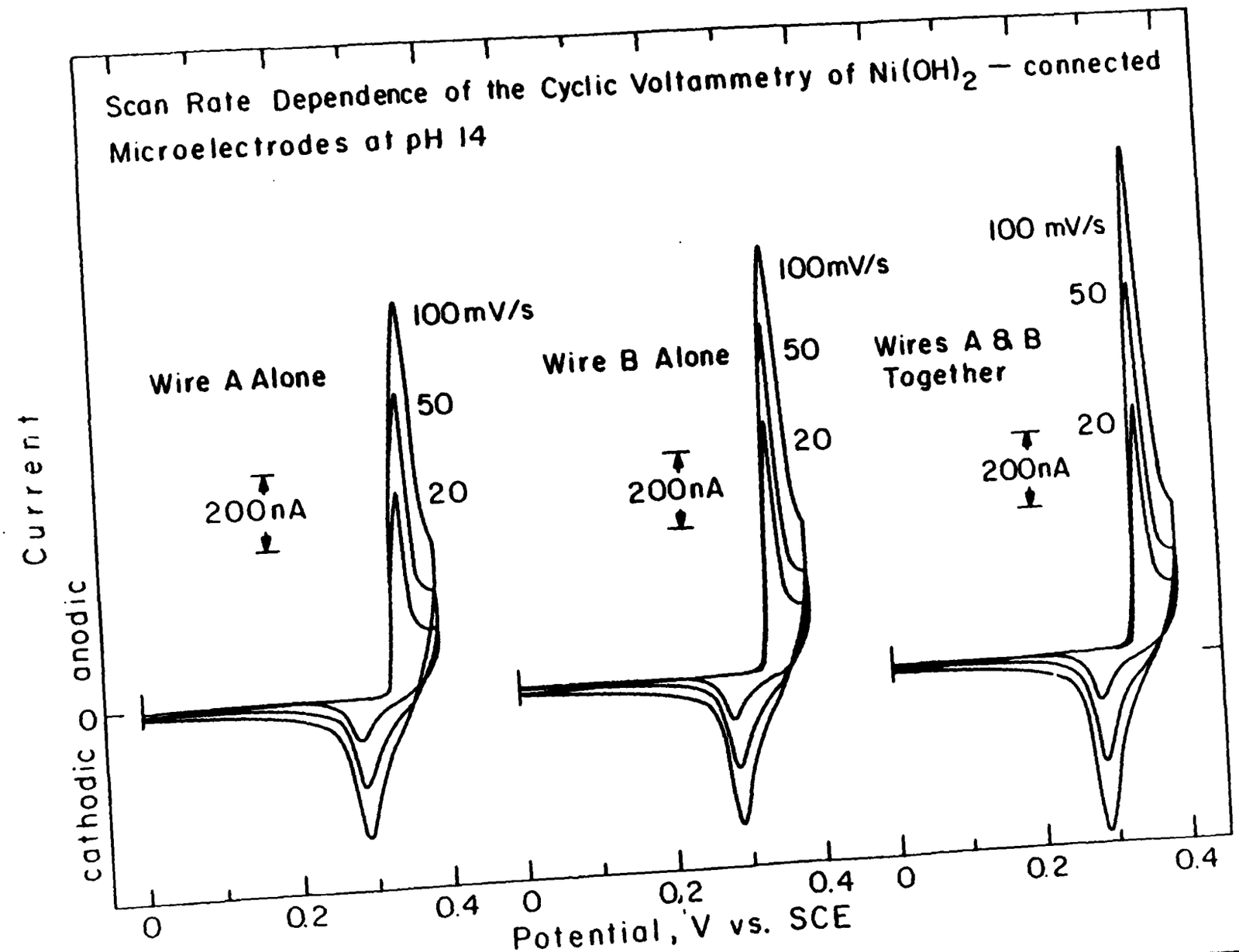
Scan Rate Dependence of the Cyclic Voltammetry of Ni(OH)2 — connected Microelectrodes at pH 14
Wire A Alone
100mV/s
50
20
200nA
Wire B Alone
100mV/s
50
20
200nA
Wires A & B Together
100 mV/s
50
20
200nA
Current
cathodic 0 anodic
0
0.2
0.4
Potential, V vs. SCE

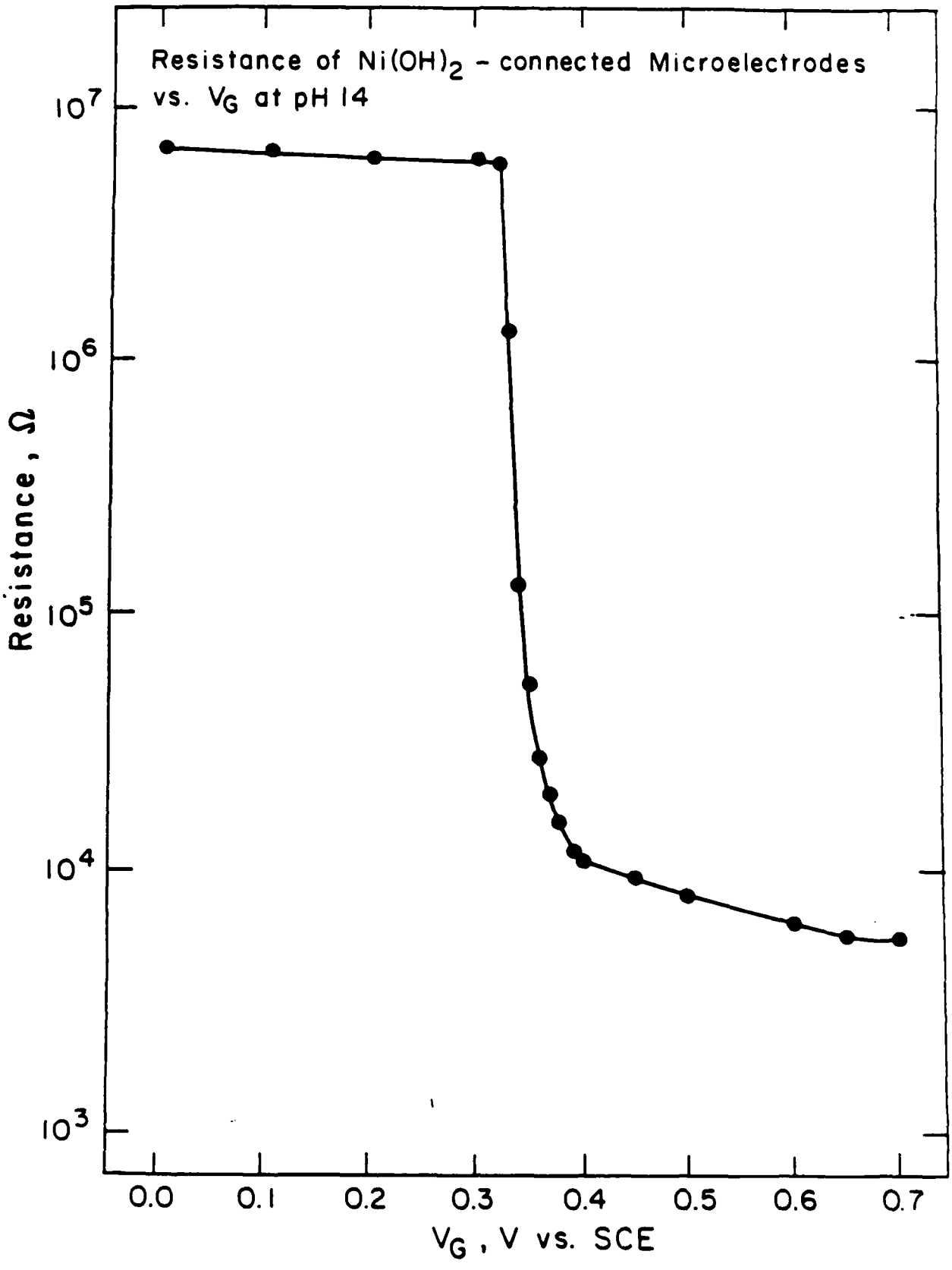
Resistance of Ni(OH)2 - connected Microelectrodes
vs. VG at pH 14
10^7
10^6
10^5
10^4
10^3
Resistance, Ω
0.0
0.1
0.2
0.3
0.4
0.5
0.6
0.7
VG, V vs. SCE

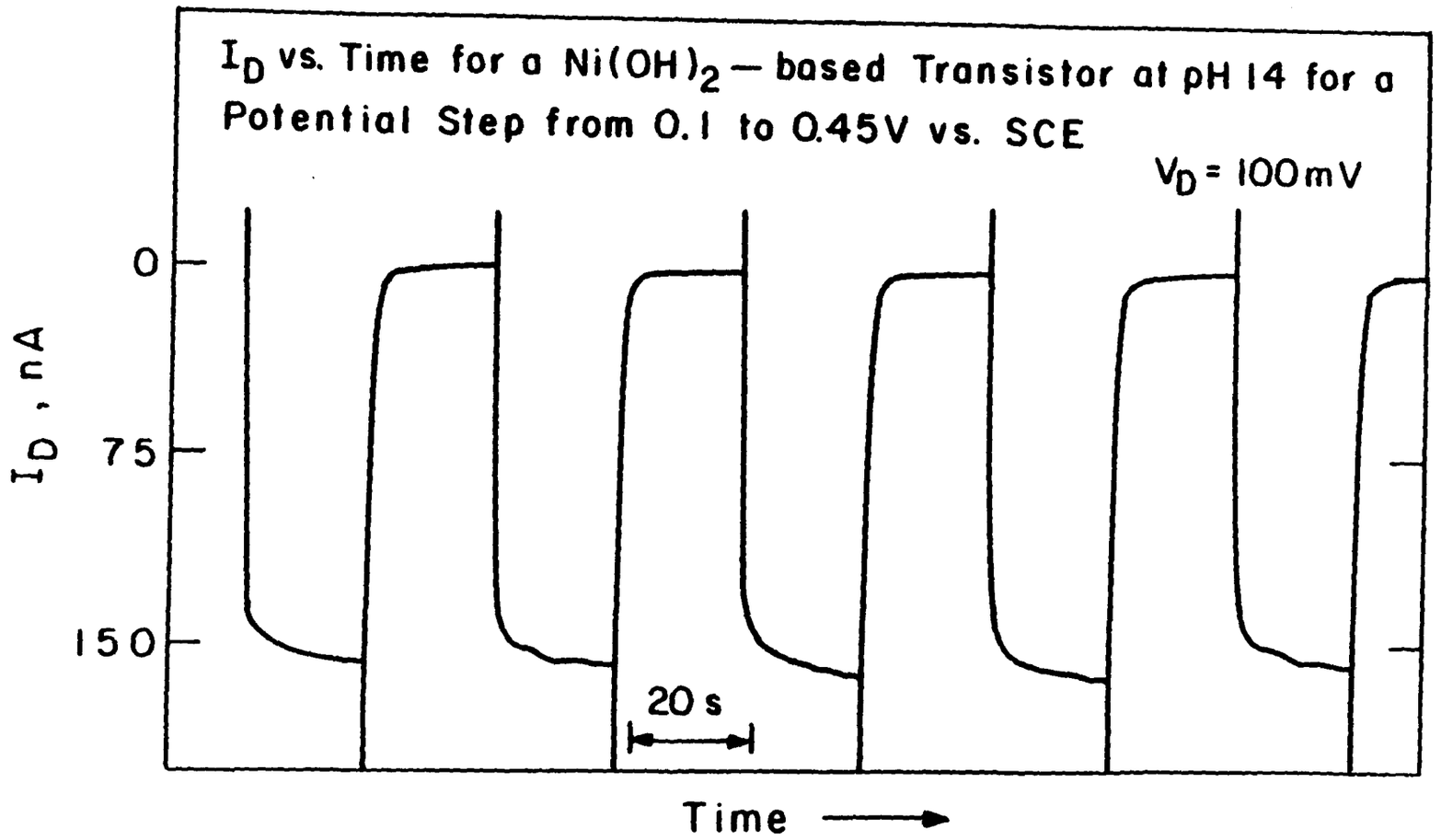
I_D vs. Time for a $Ni(OH)_2$ — based Transistor at pH 14 for a Potential Step from 0.1 to 0.45V vs. SCE
V_D = 100mV
0
75
150
I_D, nA
20 s
Time

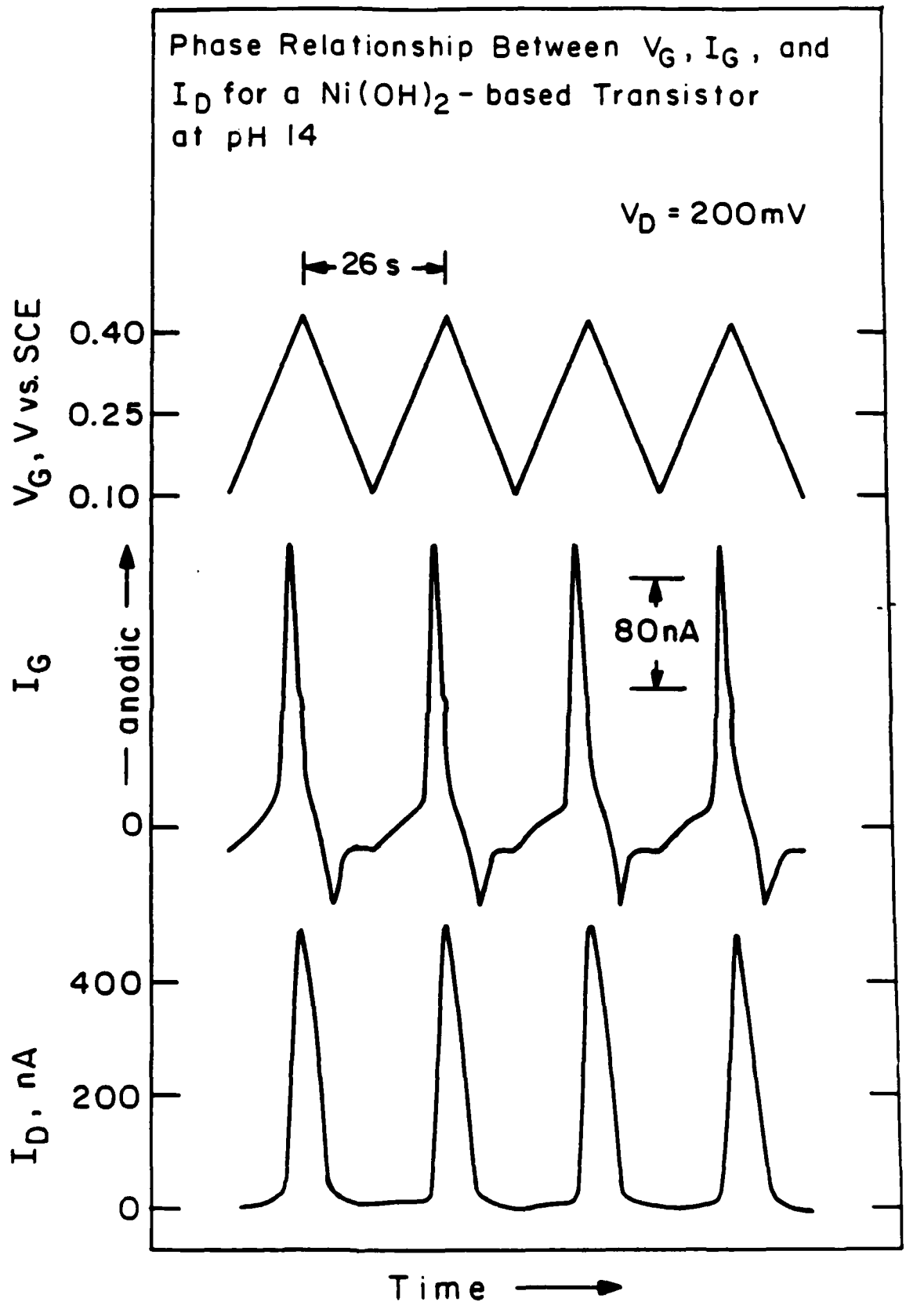
Phase Relationship Between V_G, I_G, and I_D for a $Ni(OH)_2$ - based Transistor at pH 14
V_D = 200mV
26 s
V_G, V vs. SCE
0.40
0.25
0.10
I_G
— anodic
80nA
0
I_D, nA
400
200
0
Time

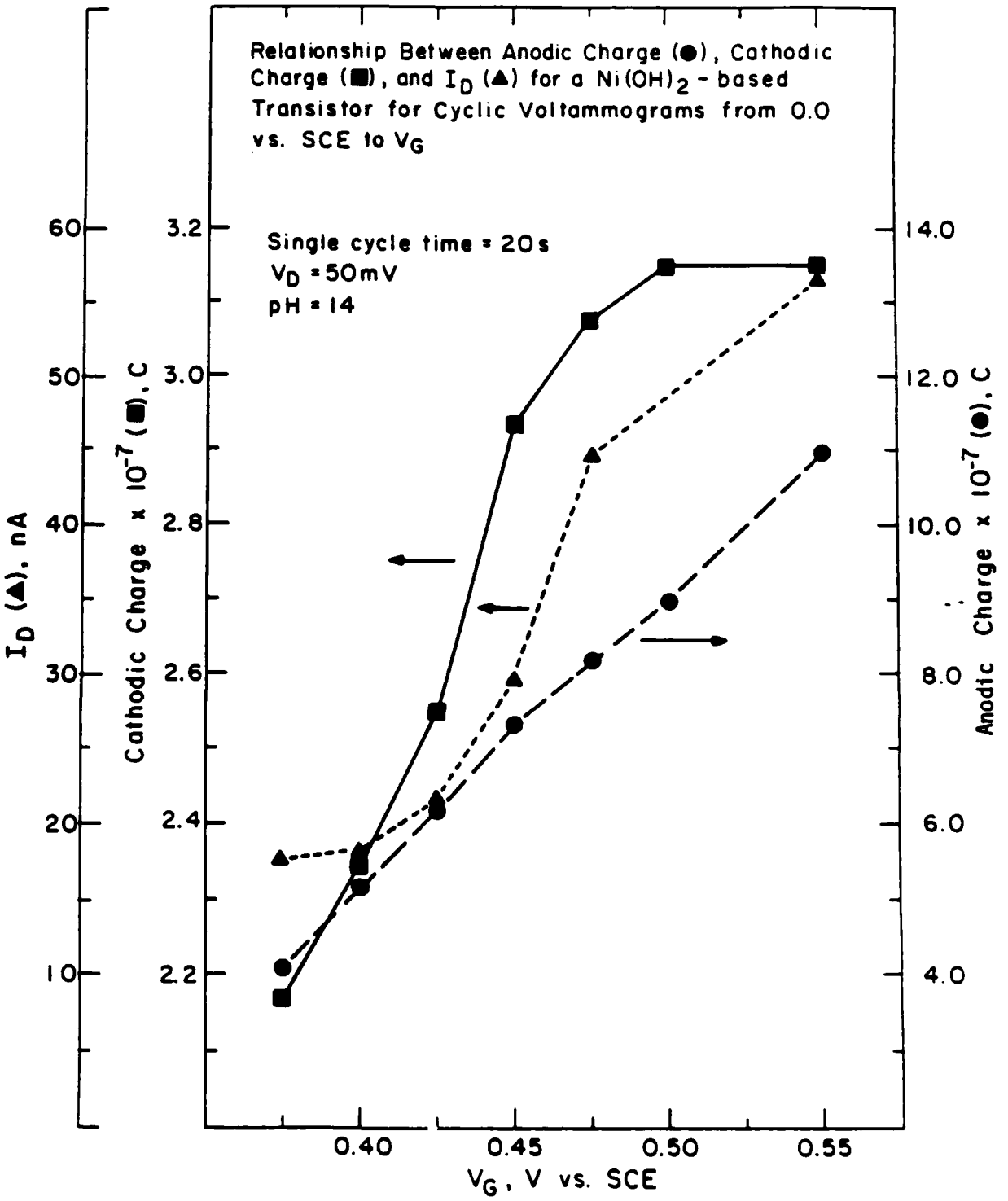
Relationship Between Anodic Charge (●), Cathodic Charge (■), and I_D (▲) for a $Ni(OH)_2$ - based Transistor for Cyclic Voltammograms from 0.0 vs. SCE to V_G
Single cycle time = 20s
V_D = 50mV
pH = 14
I_D (▲), nA
Cathodic Charge x 10^{-7} (■), C
Anodic Charge x 10^{-7} (●), C
V_G, V vs. SCE
60
50
40
30
20
10
3.2
3.0
2.8
2.6
2.4
2.2
14.0
12.0
10.0
8.0
6.0
4.0
0.40
0.45
0.50
0.55

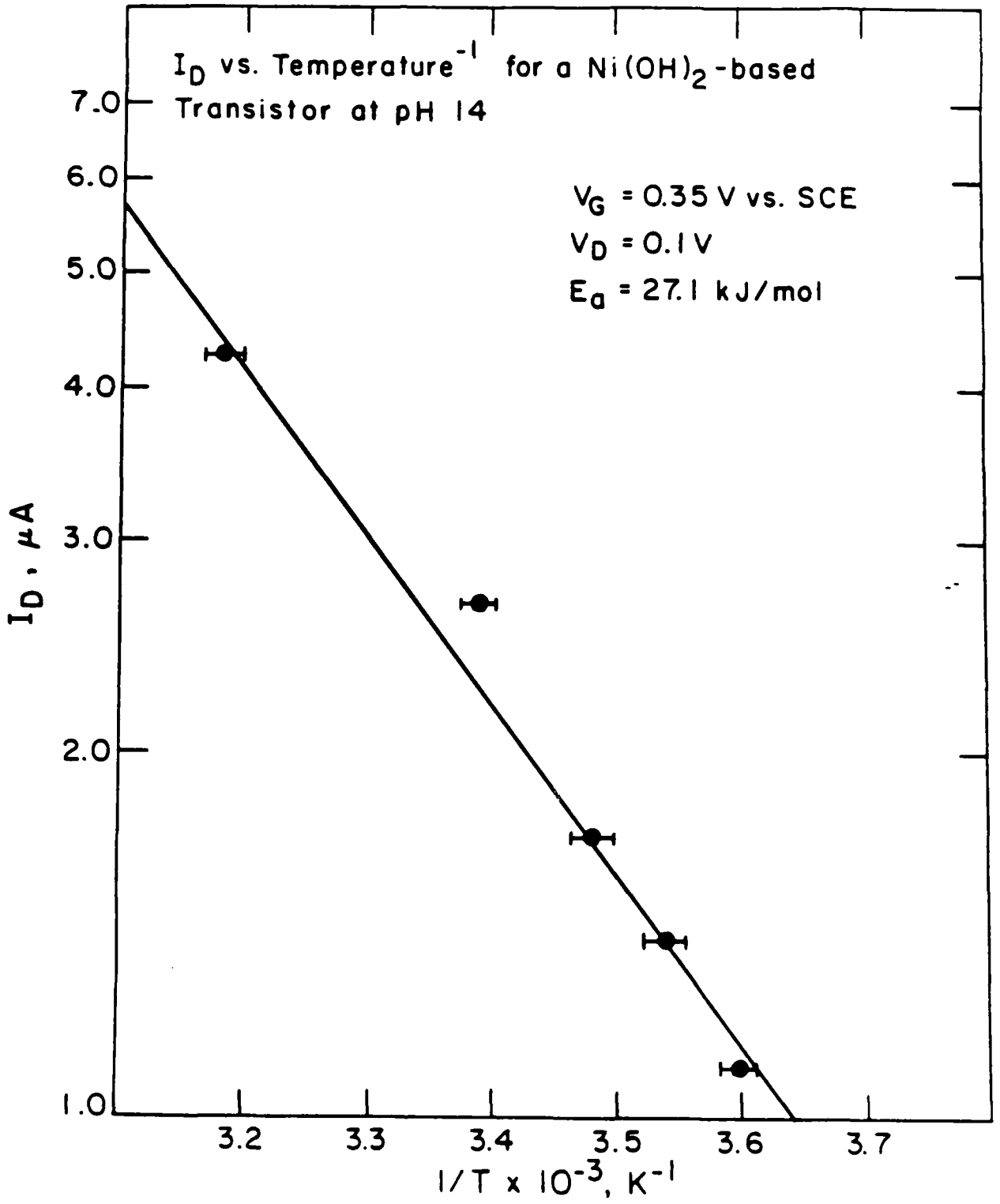
I_D vs. Temperature^{-1} for a $Ni(OH)_2$-based Transistor at pH 14
V_G = 0.35 V vs. SCE
V_D = 0.1 V
E_a = 27.1 kJ/mol
I_D, μA
7.0
6.0
5.0
4.0
3.0
2.0
1.0
3.2
3.3
3.4
3.5
3.6
3.7
1/T x 10^{-3}, K^{-1}

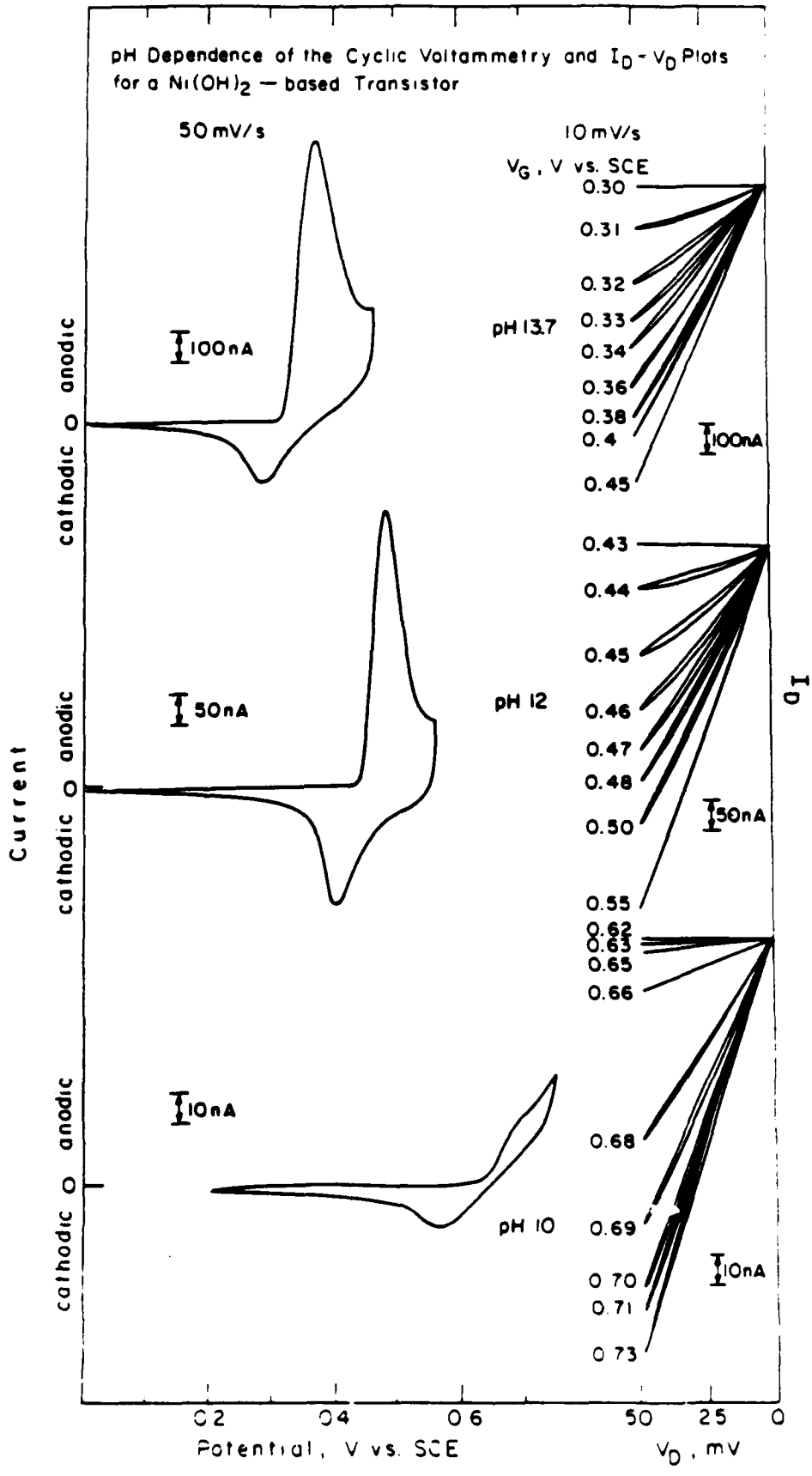
pH Dependence of the Cyclic Voltammetry and I_D - V_D Plots for a $Ni(OH)_2$ — based Transistor
50 mV/s
10 mV/s
V_G, V vs. SCE
0.30
0.31
0.32
0.33
0.34
0.36
0.38
0.4
0.45
pH 13.7
100nA
100nA
0.43
0.44
0.45
0.46
0.47
0.48
0.50
0.55
pH 12
50nA
50nA
0.62
0.63
0.65
0.66
0.68
0.69
0 70
0.71
0 73
pH 10
10nA
10nA
Current
cathodic 0 anodic
cathodic 0 anodic
cathodic 0 anodic
I_D
0.2
0.4
0.6
50
25
0
Potential, V vs. SCE
V_D, mV

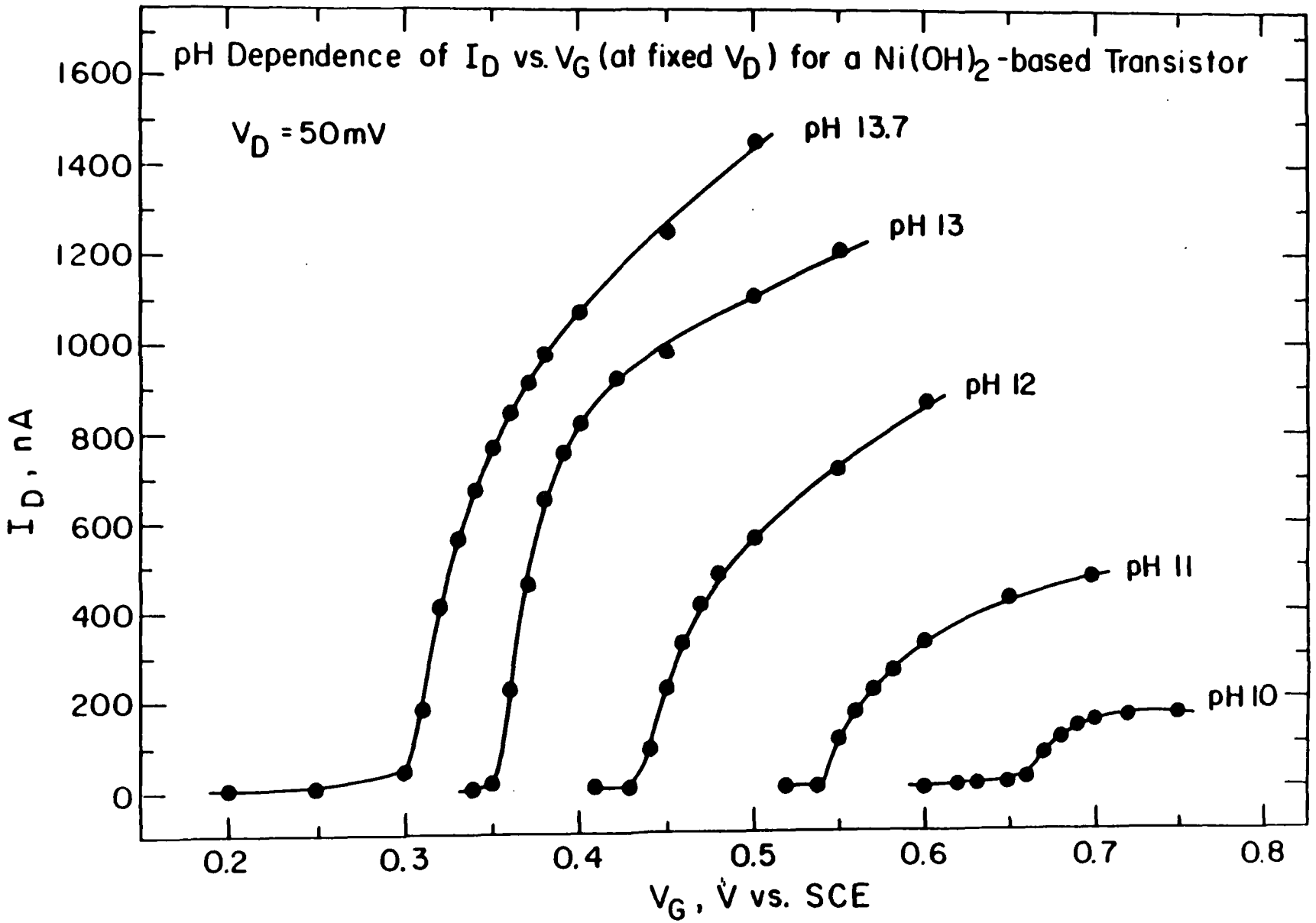
pH Dependence of I_D vs. V_G (at fixed V_D) for a $Ni(OH)_2$-based Transistor
V_D = 50mV
pH 13.7
pH 13
pH 12
pH 11
pH 10
I_D, nA
1600
1400
1200
1000
800
600
400
200
0
0.2
0.3
0.4
0.5
0.6
0.7
0.8
V_G, V vs. SCE

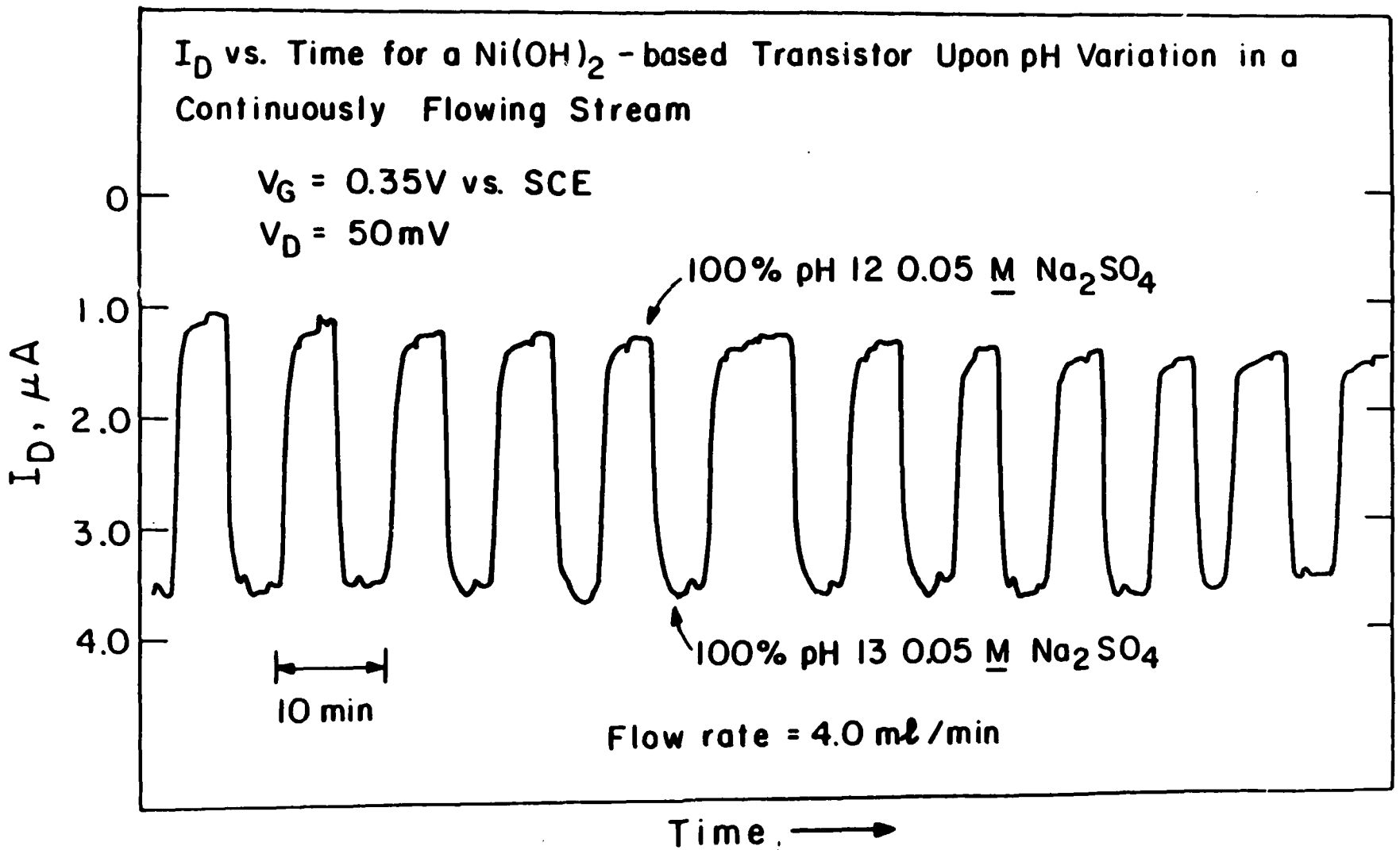
I_D vs. Time for a $Ni(OH)_2$ - based Transistor Upon pH Variation in a Continuously Flowing Stream
V_G = 0.35V vs. SCE
V_D = 50mV
100% pH 12 0.05 M Na_2SO_4
100% pH 13 0.05 M Na_2SO_4
10 min
Flow rate = 4.0 ml/min
I_D, μA
0
1.0
2.0
3.0
4.0
Time

TECHNICAL REPORT DISTRIBUTION LIST, GEN

	No. Copies
Office of Naval Research Attn: Code 1113 800 N. Quincy Street Arlington, Virginia 22217-5000	2
Dr. Bernard Douda Naval Weapons Support Center Code 50C Crane, Indiana 47522-5050	1
Naval Civil Engineering Laboratory Attn: Dr. R. W. Drisko, Code L52 Port Hueneme, California 93401	1
Defense Technical Information Center Building 5, Cameron Station Alexandria, Virginia 22314	12 high quality
DTNSRDC Attn: Dr. H. Singerman Applied Chemistry Division Annapolis, Maryland 21401	1
Dr. William Tolles Superintendent Chemistry Division, Code 6100 Naval Research Laboratory Washington, D.C. 20375-5000	1
Dr. David Young Code 334 NORDA NSTL, Mississippi 39529	1
Naval Weapons Center Attn: Dr. Ron Atkins Chemistry Division China Lake, California 93555	1
Scientific Advisor Commandant of the Marine Corps Code RD-1 Washington, D.C. 20380	1
U.S. Army Research Office Attn: CRD-AA-IP P.O. Box 12211 Research Triangle Park, NC 27709	1
Mr. John Boyle Materials Branch Naval Ship Engineering Center Philadelphia, Pennsylvania 19112	1
Naval Ocean Systems Center Attn: Dr. S. Yamamoto Marine Sciences Division San Diego, California 91232	1

DISTRIBUTION LIST

All Reports
Molecular Biology Program, Code 441MB
Office of Naval Research
800 N. Quincy Street
Arlington, VA 22217

Annual, Final and Technical Reports
Defense Technical Information Center (2 copies)
Building 5, Cameron Station
Alexandria, VA 22314

Annual and Final Reports Only (one copy each)
Scientific Library
Naval Biosciences Laboratory
Naval Supply Center
Oakland, CA 94625

Commanding Officer
Naval Medical Research & Development Command
National Naval Medical Center
Bethesda, MD 20814

Director
Infectious Disease Program Center
Naval Medical Research Institute
National Naval Medical Center
Bethesda, MD 20814

Commander
Chemical and Biological Sciences Division
Army Research Office
Research Triangle Park, NC 27709

Commander
U.S. Army Research and Development Command
Attn: SGRD-PLA
Fort Detrick
Frederick, MD 21701

Commander
USAMRIID
Fort Detrick
Frederick, MD 21701

Commander
Air Force Office of Scientific Research
Bolling Air Force Base
Washington, DC 20332

Administrative Contracting Officer
Office of Naval Research Laboratory
(address varies - obtain from Business Office)

Final and Technical Reports Only
Director, Naval Research Laboratory (6 copies)
Attn: Code 2627
Washington, DC 20375

END

1-87

DTIC